

1 **Quantification of nocturnal water use and its composition in a *Eucalyptus***
2 ***urophylla* × *E. grandis* plantation on the Leizhou Peninsula, South China**

3 **Zhichao Wang^{1,2,3}, Apeng Du^{2,3}, Siru Liu⁴, Yuxing Xu², Wankuan Zhu², Wenhua Xiang^{1*}**

4 ¹ Faculty of Life Science and Technology, Central South University of Forestry and Technology,
5 Changsha, 410004, Hunan, China

6 ² Research Institute of Fast-growing Trees (RIFT), Chinese Academy of Forestry (CAF),
7 Zhanjiang 524022, Guangdong, China

8 ³ Guangdong Zhanjiang Eucalyptus Plantation Ecosystem Research Station, Zhanjiang 524022,
9 Guangdong, China.

10 ⁴ South Subtropical Crops Research Institute, CATAS Zhanjiang, 524091, Guangdong, China.

11
12 Corresponding author: Dr. Wenhua Xiang (xiangwh2005@163.com)

13 *Faculty of Life Science and Technology, Central South University of Forestry and Technology,
14 No. 498 Southern Shaoshan Road, Changsha 410004, Hunan, China

15 Tel: +86-731-85623483; Fax: +86-731-85623483

16
17 **Key Points:**

- 18 • The nocturnal water use of *E.urophylla* × *E.grandis* accounts for about 12.35% of the
19 daily water use and therefore cannot be ignored.
- 20 • Nocturnal transpiration is driven by a combination of vapor pressure deficit, temperature
21 and humidity, with the former being predominant.
- 22 • Nocturnal water use in *E.urophylla* × *E.grandis* is mainly for nocturnal transpiration.

23

24

25 **Abstract** Nocturnal water use (Q_{night}) is an important component of the eucalyptus water
26 budget, but it has always been under-appreciated and poorly understood. To improve the
27 accuracy of water balance estimates and understanding of the nocturnal water use process in
28 eucalypts plantations, we conducted a 3-year study to investigate the characteristics of Q_{night} and
29 its components in a *Eucalyptus urophylla* × *E. grandis* plantation in southern China. The results
30 showed that the Q_{night} of *E. urophylla* × *E. grandis* was substantial and its contribution (R_{night}) to
31 daily water use (Q_{daily}) was on average 12.35%, with higher R_{night} (14.97%) in the dry season than
32 in the wet season (9.50%). However, the Q_{night} was used not only for nocturnal transpiration (Tn),
33 but also for stem refilling (Re). Tn was influenced by a combination of vapor pressure deficit
34 (VPD), air temperature (T_a) and relative humidity (RH), with VPD being the dominant driver.
35 Based on this, combined with the fact that Re was closely related to diurnal variations in
36 diameter, we have developed a novel method to distinguish Tn from Re. We found that the
37 compositional ratios of Tn and Re differed between weather conditions and months. However,
38 on a 3-year average, Q_{night} of *E. urophylla* × *E. grandis* was still mainly used for Tn (58.63%).
39 Our results highlight the non-ignorability of Q_{night} and the high variability of the compositional
40 ratios of Re and Tn, and suggest that Q_{night} and its components should be accurately quantified
41 and taken into account when studying the water balance in eucalyptus stands.

42 **Plain Language Summary** Eucalyptus is one of the world's most important fast-growing
43 tree species. Its nocturnal water use plays an important role in many physiological activities.
44 However, it has been neglected and poorly understood due to its relatively low abundance and
45 the difficulty in distinguishing its composition. We analyzed the nocturnal water use of *E.*
46 *urophylla* × *E. grandis* on the Leizhou Peninsula, South China, by using accurate monitoring
47 data collected between 2019 and 2021, and developed a novel method to distinguish the
48 components of nocturnal water use - nocturnal transpiration and stem refilling. We found that
49 nocturnal water use by *E. urophylla* × *E. grandis* was substantial, and although the proportions
50 of its two components varied greatly between weather and months, on average it was still
51 predominantly used for nocturnal transpiration, which was mainly driven by vapor pressure
52 deficit. Our results highlight the non-neglectability of nocturnal water use in eucalypt
53 hydrological budgets and the importance of accurately quantifying its components, and provide a

54 new quantification method, which can help us improve the accuracy of water budgets and our
55 understanding of nocturnal water use processes.

56 **1 Introduction**

57 Sap flow is the movement of fluid within the sapwood of the plant root, stem, or branch (Forster,
58 2014). Monitoring plant sap flow is currently recognized as an important method for
59 understanding the status of forest water use (Jonard et al., 2011; Kropp et al., 2017; Peters et al.,
60 2010). However, most of the previous sap flow research ignored night-time patterns (Hasholt,
61 1997; Jarvis, 1976). Moreover, based on the assumption that leaf stomata are completely closed
62 in the dark (Daley & Phillips, 2006; Meidner & Mansfield, 1965; Priestley & Taylor, 1972;
63 Ritchie, 1974), the multi-scale water balance estimation model assumes no sap flow at night.
64 However, numerous studies have shown that this assumption is not true in many plant species
65 (Escalona et al., 2013; Fisher et al., 2007; Rosado et al., 2012; Siddiq & Cao, 2018; Yu et al.,
66 2018). Stomata in many plant species remain partially open at night (Chowdhury et al., 2022;
67 Wu et al., 2020), which undoubtedly results in nocturnal transpiration (Daley & Phillips, 2006;
68 Wang et al., 2012). Recently, with the development of the thermal dissipation method,
69 considerable nocturnal sap flow has been reported (Barbeta et al., 2012; Forster, 2014; Han et al.,
70 2019; Rosado et al., 2012; Wu et al., 2020; Zeppel et al., 2011), and has been recognized as an
71 important factor affecting different physiological processes in trees, including nocturnal nutrient
72 transport (McDonald et al., 2002), oxygen transfer for nocturnal respiration (Fang et al., 2018;
73 Siddiq & Cao, 2018), and next-day photosynthesis, transpiration, and drought stress resistance
74 (Daley & Phillips, 2006). However, nocturnal sap flow and its composition are not well
75 understood, which hinders accurate estimation of the stand water balance and a proper
76 understanding of crown nocturnal water use processes.

77 In many tree species, the measured nocturnal sap flow does not necessarily indicate nocturnal
78 transpiration; rather, it often integrates concurrent nocturnal transpiration and the amount of
79 water required to recover from the stem water deficit caused by transpiration that occurred
80 during the previous day (Chen et al., 2020; Di et al., 2019; Liu et al., 2021; Siddiq & Cao, 2018;
81 Snyder et al., 2003; Wang et al., 2007). These two components usually overlap in time and space
82 (Di et al., 2019; Liu et al., 2021), but represent opposite directions of water use: water storage in
83 the stem and water loss to the atmosphere. Distinguishing nocturnal stem refilling (Re) and

84 nocturnal transpiration (T_n) is a key step to improve the accuracy of stand water consumption
85 estimation and to reveal mechanistic control over crown nocturnal water use. However, this has
86 always been an extremely difficult and challenging task.

87 Stem diameter of trees fluctuates periodically throughout the day, and follows a diurnal pattern,
88 with the lowest values in the afternoon and highest values in the early morning (Dietrich et al.,
89 2018; Paul et al., 2012; Vilas et al., 2019; Zweifel, 2016). This short-term diurnal variation in
90 stem size is closely related to changes in the water content of stem cells (i.e., live phloem,
91 fibrous phloem, and the live and dead cells of the phellem) caused by an imbalance between
92 transpiration and root water uptake (Chan et al., 2016; Claudia et al., 2015; Zweifel et al., 2000;
93 Zweifel et al., 2005). When transpiration is greater than the root water uptake, the tree stem loses
94 water and shrinks. On the contrary, when transpiration is lower than the root water uptake, the
95 tree stem refills and swells (Claudia et al., 2015; Zweifel et al., 2005). Thus, daily fluctuations in
96 stem diameter can reflect the diurnal rhythms of stem water storage depletion and replenishment
97 (Dietrich et al., 2018; Jiménez et al., 2019). Investigating the dynamic changes in nocturnal
98 forest diameter provides a feasible method to screen out time periods without R_e . This provides a
99 way to exclude the confounding effect of R_e and thus establish a highly explanatory model for
100 estimating T_n using its drivers. This model could be used to separate T_n from R_e at any given
101 time.

102 Understanding the factors that influence T_n will provide a strong foundation for developing a T_n
103 prediction model. The drivers of T_n can be determined by analyzing the relationship between
104 nocturnal sap flow and potential influencing factors (Doronila & Forster, 2015; Zeppel et al.,
105 2010). Previous studies have investigated the drivers of T_n in trees. However, they have come to
106 different conclusions (Chen et al., 2020; Chowdhury et al., 2022; Di et al., 2019, 2022; Rosado et
107 al., 2012; Sellin & Lubenets, 2010). For example, Siddiq & Cao (2018) found that VPD was the
108 driver of T_n in 18 broadleaf species in a tropical seasonal climate and was independent of wind
109 speed (WS). In contrast, a study by Wu et al. (2020) on T_n of *Acer truncatum* in Beijing
110 concluded that a combination of VPD and wind speed better explained T_n , and this finding has
111 also been observed in many studies (Benyon, 1999; Daley & Phillips, 2006; Phillips et al., 2010).
112 In a study of T_n in two temperate evergreen tree species, Zeppel et al. (2010) concluded that in
113 addition to VPD and WS, soil moisture content (SWC) had a significant positive effect on T_n .

114 However, in a study of two tree species in semi-arid regions, Chen et al. (2020) found that
115 nocturnal sap flow in the middle-aged *Pinus tabuliformis* stand and the young *Acer truncatum*
116 stand was significantly negatively correlated with SWC, whereas the young *Pinus tabuliformis*
117 stand and the middle-aged *Acer truncatum* stand was not correlated with SWC. Furthermore,
118 numerous studies have also observed strong correlations between atmospheric temperature (Ta)
119 and relative humidity (RH) and nocturnal sap flow (Fisher et al., 2007; Sellin & Lubenets, 2010;
120 Wang et al., 2012). Different findings suggest that the drivers of Tn may vary considerably
121 among plant species, site conditions, ecosystem types and climates (Chen et al., 2020;
122 Chowdhury et al., 2022; Wu et al., 2020). To date, the drivers of Tn in eucalyptus under the
123 marine monsoon climatic conditions in China are still unclear, which hinders further
124 understanding of the mechanistic controls on nocturnal water use by eucalyptus in China.

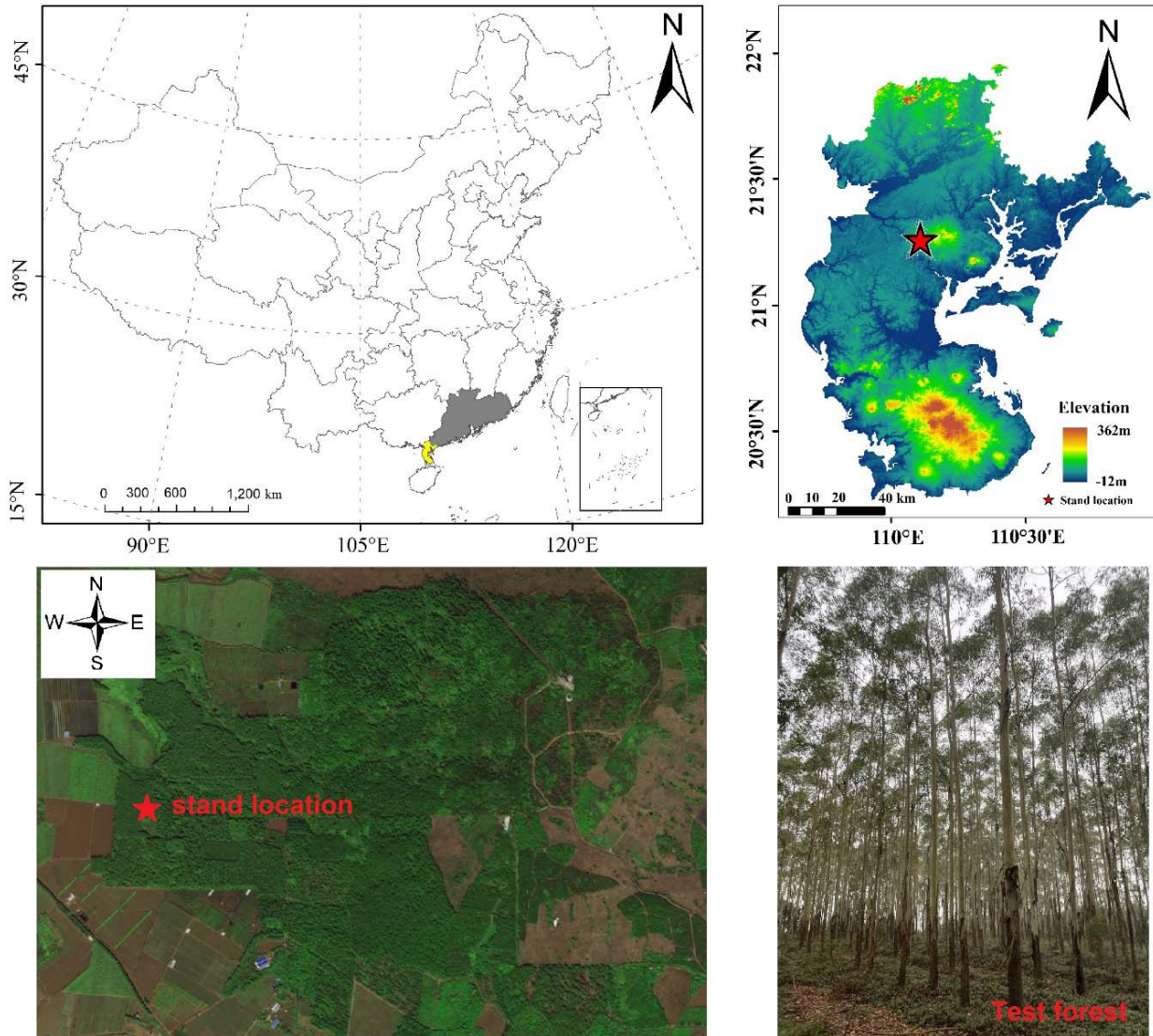
125 Eucalyptus is an exotic, fast-growing and high-yielding tree species planted in southern China.
126 The planted area has reached 5,467,400 ha (Arnold et al., 2020). However, the rapid expansion
127 of its plantation area in southern China has raised concerns about the impacts on regional water
128 resource security (Engel et al., 2005; Liu et al., 2017). In order to properly assess and predict the
129 ecological and hydrological impacts of eucalyptus plantations in the context of global climate
130 change, an accurate understanding of their diurnal water use patterns and control mechanisms is
131 required. However, nocturnal water use in eucalyptus plantations has often been overlooked due
132 to its low proportion. Although some studies have been conducted in Australia, the country of
133 origin (Benyon, 1999), the patterns of nocturnal water use are bound to be quite different, as the
134 eucalyptus species and the climatic conditions of the eucalyptus growing areas in China are quite
135 different. Therefore, an in-depth study of the nocturnal sap flow and its components in
136 eucalyptus plantations in China is crucial. *E. urophylla* × *E. grandis* is the most representative
137 eucalyptus species in China, accounting for approximately one-third of the total eucalyptus
138 plantation area. Therefore, this study aimed to: (1) investigate the seasonal dynamics of
139 Q_{daily} , Q_{night} and R_{night} of *E. urophylla* × *E. grandis*; (2) determine the main drivers of Tn in the *E.*
140 *urophylla* × *E. grandis* plantation and distinguish Tn and Re from nocturnal sap flow; and (3)
141 examine the daily and seasonal variation in the distribution ratios of Tn and Re.

142 2 Materials and Methods

143 2.1 Experimental site and plantation

144 This study was conducted at the Zhanjiang Eucalyptus Plantation Ecosystem Research Station
145 (21°16'N, 110°05'E) in Leizhou Peninsula, Guangdong, China (Figure1). The terrain is flat with
146 low hills, with elevations ranging from 80-220.8 m above sea level. According to the long-term
147 meteorological records (1980-2020) of the weather station in this area, the region experiences a
148 maritime monsoon climate, with an average annual precipitation of approximately 1,760.9 mm,
149 77–85% of which occurs in the wet season (May–October). The mean annual temperature is
150 23.1°C (minimum 1.4°C in January, and maximum 38.1°C in July), and the annual RH is 80.4%
151 (Xu et al., 2020). The soil is classified as Rhodi-Udic Ferralosols, according to World Reference
152 Base for Soil Resources (IUSS Working Group WRB, 2006), which developed from weathered
153 sediments of basalt. The soil is acidic, with a mean pH of 5.7 at 0–100 cm depth.

154 In 2019, we selected an *E. urophylla* × *E. grandis* plantation, which was established in July 2012
155 with clone DH32-29 for long term experiment. Trees were planted by digging holes at a density
156 of 1,666 trees·ha⁻¹. At the beginning of the experiment (2019), the mean diameter at breast
157 height (DBH; 1.3 m) was 14.9 cm and mean height was 16.6 m. The mean leaf area index (LAI)
158 of the stand was 1.78. The physico-chemical properties of the soils at the test site are shown in
159 Table 1. The understory shrub vegetation in the selected experimental plots consisted mainly of
160 *Schefflera octophylla*, *Mallotus apelta*, *Common lantana* and *Melastoma candidum*. The
161 herbaceous layer is relatively rich and consists mainly of *Bidens pilosa*, *Euphorbia hirta*,
162 *Chromolaena odorata* and *Digitaria sanguinalis*.



163

164 **Figure 1.** Location of study area and the *Eucalyptus urophylla* × *E. grandis* plantation planted in
 165 2012 in Leizhou Peninsula, Guangdong, China.

166

167 **Table 1**

168 *Basic Physical and Chemical Properties of the Soils at the Test Site.*

Indicator	Soil depth(cm)				
	0-20	20-40	40-60	60-80	80-100
pH	5.44(0.14)	5.89(0.09)	5.82(0.06)	5.82(0.02)	5.65(0.06)
BD (g.m ⁻³)	1.02(0.03)	1.13(0.02)	1.34(0.02)	1.37(0.03)	1.30(0.01)

SOM (%)	2.37(0.21)	1.47(0.15)	1.29(0.06)	0.90(0.08)	0.91(0.15)
TN(g·kg ⁻¹)	1.36(0.07)	1.08(0.02)	0.93(0.02)	0.82(0.02)	0.67(0.03)
TP(g·kg ⁻¹)	0.94(0.11)	0.77(0.04)	0.84(0.04)	0.75(0.05)	0.78(0.05)
TK(g·kg ⁻¹)	4.12(0.53)	3.46(0.32)	3.80(0.59)	4.16(0.93)	4.40(0.45)
AN (mg·kg ⁻¹)	335.23(13.59)	319.22(36.60)	334.31(20.06)	265.48(14.16)	216.78(22.59)
AP (mg·kg ⁻¹)	2.37(0.56)	2.92(0.32)	4.8(0.79)	2.81(0.35)	5.42(0.16)
AK (mg·kg ⁻¹)	18.20(2.91)	15.22(1.14)	12.48(1.16)	12.38(0.30)	14.52(0.88)

169 **Note:** BD, bulk density; SOM, soil organic matter; TN, total nitrogen; TP, total phosphorus; TK,
 170 total potassium; AN, available nitrogen; AP, available phosphorus; AK, available potassium.
 171 Values in parentheses represent standard errors of three replicate plots in the *E. urophylla* × *E.*
 172 *grandis* plantation.

173 2.2 Meteorological factors and soil water content measurement

174 Meteorological factors were continuously monitored using an automatic meteorological
 175 observation system set up in an open area near the eucalyptus plantation. Among the
 176 meteorological parameters, Ta (°C) and RH (%) were measured with a thermo recorder
 177 (HMP155A, Vaisala, Helsinki, Finland); the solar radiation (Rs, W·m⁻²) was measured by a
 178 photon sensor (LI-200R, LICOR, Lincoln, NE, USA); wind speed (WS; m·s⁻¹) was measured
 179 with an anemometer (ATMOS 22, Decagon, Pullman, WA, USA); and precipitation (P; mm)
 180 measured with a tilting rain gauge (TE525MM, Campbell, Logan, UT, USA). All meteorological
 181 data were collected at 1 min intervals, averaged every 10 min, and recorded using a data logger
 182 (CR3000; Campbell, USA). The vapor pressure deficit (VPD, kPa) was calculated from Ta and
 183 RH according to the following equation (Campbell & Norman, 1998):

$$184 \quad \text{VPD} = 0.611 \times e^{\frac{17.502T_a}{T_a + 240.97}} \times (1 - \text{RH}) \quad (1)$$

185 Soil water content (SWC) was measured using six soil moisture sensors (CS616, Campbell,
 186 Logan, UT, USA) installed near the sap flow monitoring sample trees at different soil depths (10,
 187 20, 40, 60, 80 and 100 cm). Measurements were recorded every 30 min by a data logger
 188 (CR1000, Campbell, Logan, UT, USA) synchronized with sap flow monitoring of the trees as
 189 described below.

190 2.3. Sap flow estimation methods and sapwood area determination

191 Six trees that cover the DBH range in the plantation (Table 2) were selected each year to
 192 measure sap flow (Di et al., 2019; Han et al., 2019; Pei et al., 2023). This sampling strategy, as
 193 indicated by the close correspondence between the biometric characteristics of the sap flow
 194 sampled trees and the stand, was satisfactory in representing the individual variability of the
 195 stand under study (Chen et al., 2020). In particular, only trees with symmetric stems and no
 196 branch or bark defects within 15 cm above or below breast height (1.3m) were selected (Chen et
 197 al., 2020).

198 The sap flow density ($\text{cm}\cdot\text{min}^{-1}$) of sample trees was monitored continuously from January 2019
 199 to December 2021 using thermal dissipation probes (TDP) (SF-G; Ecomatik, Munich, Bavaria,
 200 Germany). To ensure accurate determination of sap density, and thus a more accurate distinction
 201 between Tn and Re, four TDP probes were inserted into the active xylem of each sample tree in
 202 four directions from south-east to north-west at trunk height at breast height (1.3 m) to avoid
 203 differences in the direction of sap flow in the sample trees, and covered with radiation-shielding
 204 aluminum foil to avoid solar radiation and reduce the effects of ambient temperature fluctuations
 205 and rain. The connection between S_0 (heated probe) and S_1 (reference probe) provides the
 206 difference in their temperature (ΔT), which was recorded at 30 min intervals using the data
 207 logger (CR1000; Campbell, USA). Then, the ΔT was converted into sap flow density, based on
 208 the calibration equation (Granier, 1987):

$$209 \quad J_d = 0.714 \times \left(\frac{\Delta T_{max} - \Delta T}{\Delta T} \right)^{1.231} \quad (2)$$

210 where J_d is the sap flow density in one direction of the measured tree ($\text{cm}\cdot\text{min}^{-1}$), and ΔT_{max} is
 211 the maximum ΔT when the xylem sap flow density is near zero. However, since the sap flow
 212 density cannot reach zero every day, the maximum value of ΔT obtained over a period of 7–10
 213 days was considered as ΔT_{max} to avoid underestimating the nocturnal sap flow (Lu et al., 2004).
 214 Ultimately, the sap flow density of the measure tree was averaged over four directions.

215 Calculating the water consumption of trees through sap flow density requires the data of their
 216 sapwood area (SA, cm^2). Assuming circular stem cross-sections, individual values of SA were
 217 calculated by measuring the heartwood and sapwood thickness of 18 non-sample trees per DBH
 218 class in the experimental forest, and then the cross-section at breast height was measured by

219 felling. The color difference between sapwood and heartwood was used to identify their
 220 boundaries. Based on the SA and DBH data of 18 trees, the empirical power function between
 221 SA and DBH of the test stand was established as follows (Figure S1):

$$222 \quad SA=0.3519 DBH^{2.018}, R^2=0.965, P<0.0001 \quad (3)$$

223 The tree water use (Q) at stand level was calculated as follows (Kumagai et al., 2005):

$$224 \quad Q = \sum J_C \left(\frac{SA_{plot}}{A_E \times 1000} \right) \times 30 \quad (4)$$

225 where Q (mm) is the total water use in a certain time period; J_C ($\text{cm} \cdot \text{min}^{-1}$) is the stand mean sap
 226 flow density which was computed as the sapwood area weighted average of sap flow density for
 227 each DBH class, 30 is the recording interval of sap flow density in minutes; SA_{plot} (cm^2) is the
 228 total SA of all trees in the experimental plot; and A_E (m^2) is the area of the experimental plot.

229 **Table 2**

230 *Details of the Sample Trees of E. urophylla × E. grandis Used in Each Year for Measuring Sap*
 231 *Flow.*

Year	Sample tree number	DBH (cm) ^a	Tree height (m)	Crown width (m×m) ^b	Sapwood area (cm ²)
2019	1	12.1	14.3	2.5×3.0	53.89
	2	13.7	14.6	3.2×3.5	69.23
	3	14.9	15.4	2.8×3.7	82.02
	4	15.5	15.3	3.1×3.8	88.82
	5	16.2	16.1	3.2×3.6	97.10
	6	17.2	17.6	3.8×4.0	109.58
2020	1	13.6	15.7	2.4×3.5	68.22
	2	14.6	19.3	3.7×3.5	78.72
	3	15.7	20.6	3.9×4.0	91.15
	4	16.5	19.4	3.5×3.2	100.76
	5	17.8	20.0	4.4×3.9	117.43
	6	18.5	20.2	4.8×3.2	126.93
2021	1	14.2	18.7	3.0×2.9	74.43
	2	16.0	19.0	3.7×3.5	94.70

3	16.6	20.4	3.6×3.0	102.00
4	17.6	20.3	3.3×3.6	114.78
5	18.7	21.0	4.1×4.6	129.72
6	20.9	20.2	5.6×5.9	162.36

232 ^aDBH, diameter at breast height.

233 ^bCrown width indicates measurements taken in east-west direction × north-south direction.

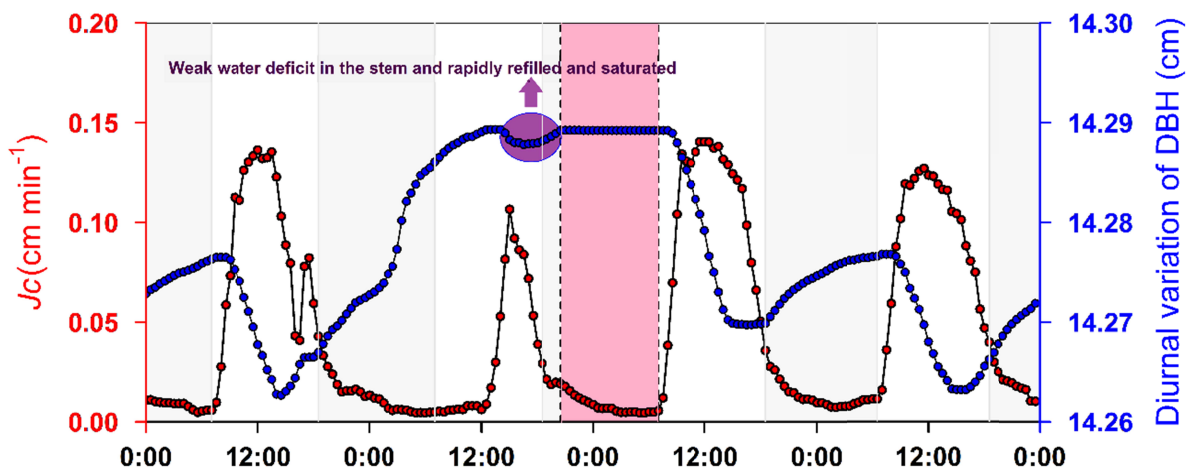
234 **2.4. Measurement of diurnal variation in DBH**

235 A circumference dendrometer (DC3; Ecomatik, Germany) was installed on the northeast side of
 236 the stem of each sample tree at 1.3 m height to measure the variation in stem circumference,
 237 which in turn converted into the variation in stem diameter. The installation of sensors at the
 238 same height minimized the potential effects of vertical variation in stem swelling and shrinking.
 239 Each sensor was mounted using a stem embracing cable wire, which consisted of a special
 240 material (purpose-specific alloy) with the lowest thermal expansion coefficient available.
 241 Pressure was applied to the sensors through the stem embracing wire to generate change in
 242 resistance for measuring stem diameter variation. The measuring range of the sensor was 25mm,
 243 and the measuring accuracy was $\pm 3.3 \mu\text{m}$. Data were recorded every 30 min with a datalogger
 244 (CR1000; Campbell, USA).

245 **2.5 The method of partitioning nocturnal sap flow**

246 The nocturnal sap flow was partitioned into Re and Tn using the following method. First, several
 247 representative days were selected in each year, when daytime transpiration was weak due to
 248 cloudiness or rain, resulting in no stem water deficit or little stem water deficit but can filling to
 249 saturate it quickly, while considerable VPD exists at night, implying that sufficient transpiration
 250 driving force exists at night (Chowdhury et al., 2022; Di et al., 2019, 2022). Figure 2 shows the
 251 continuous variation of sap flow and DBH on one of the selected typical special days. Since the
 252 short-term change in diameter was shown to be proportional related to changes in the volume of
 253 water within the stem tissues (Corell et al., 2019; Vilas et al., 2019; Xue et al., 2022; Zweifel et
 254 al., 2000, 2016), we can determine the state of stem water deficit by making high-precision
 255 observations of diameter. For example, during the red cover period in Figure 2, stem diameter
 256 reached a short-term maximum, representing a period when stem water reached saturation,

257 resulting in an inability for the stem refill at night and therefore the diameter to remain stable
 258 (Dietrich et al., 2018; Herzog et al., 1995). The sap flow density monitored during this period
 259 was considered as the nocturnal transpiration rate. Conversely, during the grey cover period in
 260 Figure 2, stem diameter did not reach its maximum value at saturation, implying that the stem
 261 was in a state of water deficit (Dietrich et al., 2018; Zweifel et al., 2001). The diameter was still
 262 increasing due to continuous Re. The sap flow monitored during this period was used for both Tn
 263 and Re. Subsequently, we used the sap flow density during the nocturnal stem saturation period
 264 to establish a high explanatory fitted equation with Tn drivers to obtain a predictive model for
 265 Tn. This model, combined with the nocturnal environmental factors, allowed us to calculate the
 266 Tn rate for any given time. The difference between the actual measured nocturnal sap flow
 267 density and the calculated Tn rate is the Re rate.



268

269 **Figure 2.** An example of a selected special day with diurnal variation in J_C and DBH. The gray-
 270 covered area is the period when the stem has a water deficit at night and is being refilled, when
 271 the monitored sap flow represents both stem refilling and nocturnal transpiration. The red
 272 covered area is the period when the stem reaches saturation and cannot be refilled, when the
 273 monitored sap flow represents only nocturnal transpiration.

274 2.6 Statistical Analyses

275 One-way analysis of variance (ANOVA) was used to examine the differences in diurnal and
 276 nocturnal environmental factors and water use as well as differences in Re ratios, soil moisture
 277 Q_{daily} , Q_{day} and R_{night} between the dry and wet seasons. Linear regression analysis was performed

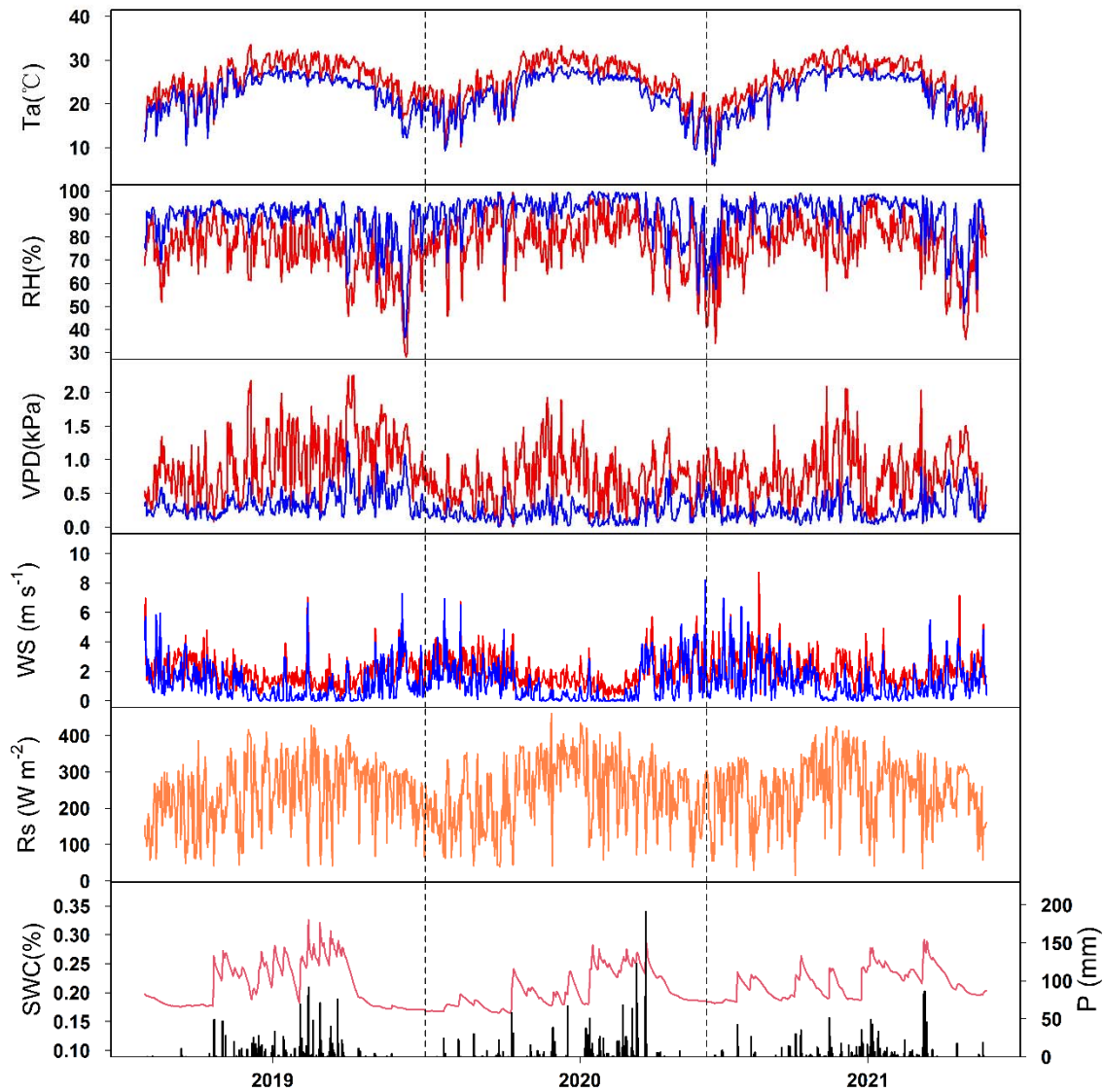
278 to examine the response of nocturnal J_c to different environmental factors, and the
279 correspondence between the measured and predicted T_n values. Regression was used to fit a
280 power function curve and a polynomial curve to quantify the relationship between SA and DBH
281 and the relationship between Re and nocturnal diameter increase, respectively. Stepwise
282 regression analysis was performed with 5% and 10% confidence levels as the threshold values
283 for selection and rejection, respectively, to develop a multivariate linear model of T_n and VPD,
284 T_a , RH and their interactions. Nighttime and daytime were defined as periods when the solar
285 radiation was less and more than $5.0 \text{ W}\cdot\text{m}^{-2}$, respectively (Di et al., 2019; Wang et al., 2012).
286 The R statistical program 4.2.2 (R Development Core Team 2022) was used to perform all
287 statistical analyses and generate the figures.

288 **3 Results**

289 **3.1 Variations in environmental conditions**

290 Daily climate variables over the 3-year experimental period showed a similar interannual
291 variability as well as seasonal variations (Figure 3). The mean daily R_s was $241.99 \text{ W}\cdot\text{m}^{-2}$ in
292 2019, $241.96 \text{ W}\cdot\text{m}^{-2}$ in 2020 and $249.48 \text{ W}\cdot\text{m}^{-2}$ in 2021. Due to the lack of typhoon rains in
293 recent years, the total annual P during the monitoring period was lower than the long-term
294 average, with 1319.5 mm in 2019, 1579.4 mm in 2020, and only 1208.4 mm in 2021. In all three
295 years, more than 80% of the P occurred between May and October (rainy season) (Figure 3). Due
296 to the influence by P, the mean daily SWC was lower ($P < 0.001$) in each dry season (18.97%,
297 18.43% and 20.27% in 2019, 2020, and 2021, respectively) than in the corresponding wet season
298 (23.75%, 22.24%, and 22.99%). The mean daytime T_a was 25.67°C in 2019, 24.99°C in 2020,
299 and 25.16°C in 2021, which were significantly greater ($P < 0.001$) than the corresponding
300 nighttime values. Similar patterns were also found for VPD and WS (Figure 3). RH, however,
301 showed a completely opposite pattern of magnitude. The mean daytime RH (73.37%, 79.73%
302 and 76.77% in 2019, 2020 and 2021, respectively) was extremely significantly lower ($P < 0.001$)
303 than the corresponding nighttime values (86.45%, 91.36% and 88.87%) (Figure 3).

304

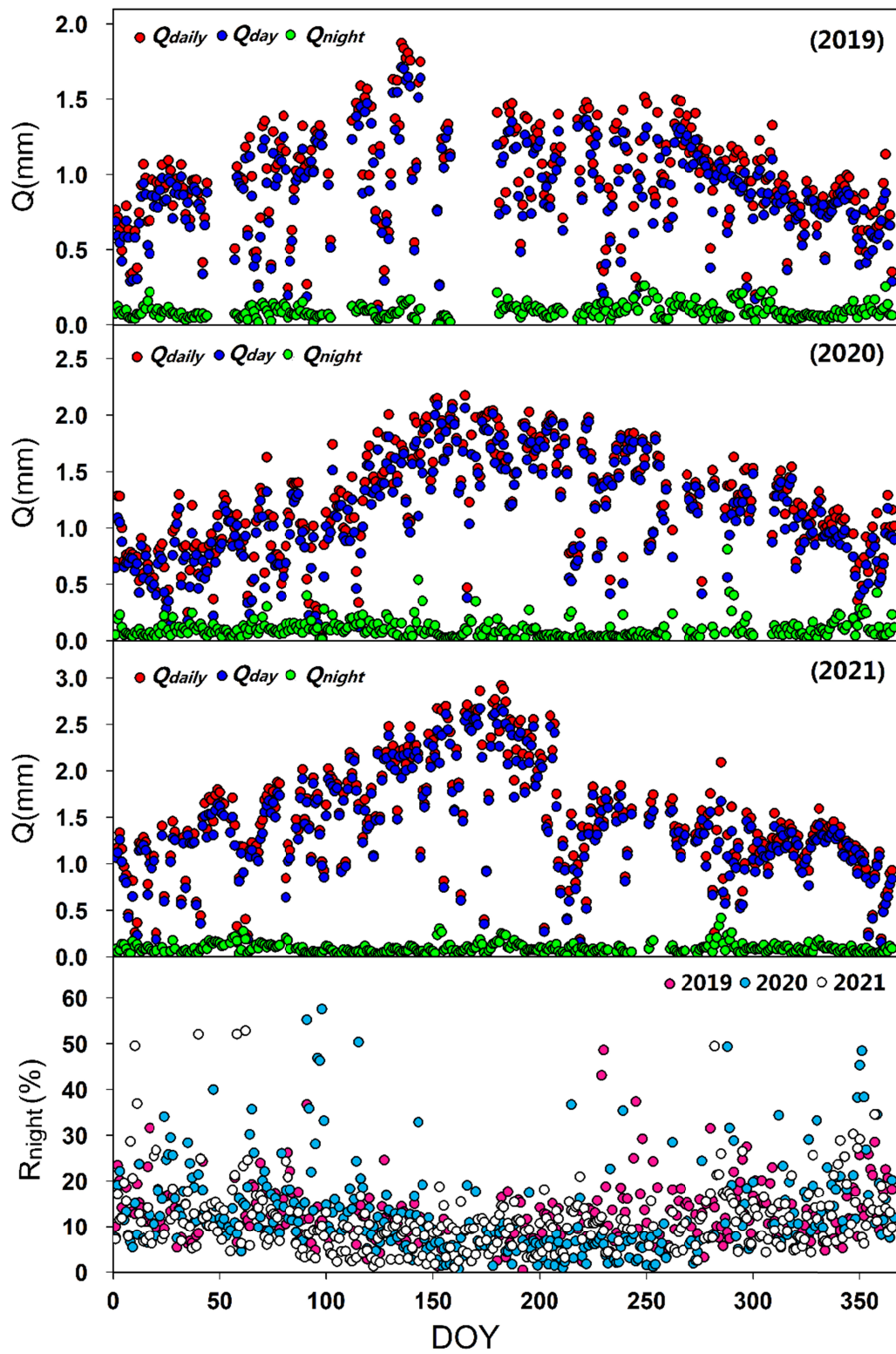


305

306 **Figure 3.** Changes in environmental variables at the experimental sites in 2019, 2020 and 2021.
 307 Here P, Ta, Rs, WS, SWC, RH and VPD represent precipitation (mm), air temperature (°C),
 308 solar radiation ($W \cdot m^{-2}$), wind speed ($m \cdot s^{-1}$), soil water content (%), relative humidity (%) and
 309 vapour pressure difference (kPa), respectively. The red lines in Ta, WS, RH and VPD represent
 310 daytime mean values, while the blue lines represent nighttime mean values. And the lines in Rs
 311 and SWC represent daily mean values. The bars in P represent the daily cumulative precipitation.

312 **3.2 Seasonal variation in Q_{daily} , Q_{day} , Q_{night} and R_{night}**

313 The pattern of seasonal and interannual variation in Q_{daily} and Q_{day} was similar, with a single peak
314 value appearing in May-July (Figure 4). The mean values of Q_{daily} (1.10mm·d⁻¹ in 2019, 1.55
315 mm·d⁻¹ in 2020 and 1.73 mm·d⁻¹ in 2021) and Q_{day} (0.99 mm·d⁻¹ in 2019, 1.45mm·d⁻¹ in 2020 and
316 1.63 mm·d⁻¹ in 2021) in the wet season were significantly higher ($P<0.001$) than the concurrent
317 average Q_{daily} (0.88 mm·d⁻¹ in 2019, 0.94 mm·d⁻¹ in 2020 and 1.25 mm·d⁻¹ in 2021) and Q_{day} (0.79
318 mm·d⁻¹ in 2019, 0.82 mm·d⁻¹ in 2020 and 1.16 mm·d⁻¹ in 2021) in the dry season. The annual
319 mean Q_{daily} was 0.98 mm·d⁻¹ in 2019, 1.23 mm·d⁻¹ in 2020, and 1.49mm·d⁻¹ in 2021. The
320 concurrent Q_{day} was 0.89 mm·d⁻¹ in 2019, 1.12 mm·d⁻¹ in 2020, and 1.39 mm·d⁻¹ in 2021, and was
321 significantly higher ($P<0.001$) than the Q_{night} value (0.124 mm·d⁻¹ in 2019, 0.159 mm·d⁻¹ in 2020,
322 and 0.171 mm·d⁻¹ in 2021). There was no obvious tendency in the seasonal variation of Q_{night} .
323 The R_{night} (Q_{night}/Q_{daily}) ranged from 0.5% to 57.6% throughout the study period, with mean
324 values of 12.66% in 2019, 12.96% in 2020, and 11.43% in 2021. The R_{night} followed a seasonal
325 trend, first decreasing and then increasing, with the mean values in the dry season (14.9% in
326 2019, 16.9% in 2020, and 13.1% in 2021) being significantly greater ($P<0.001$) than the mean
327 values in the wet season (10.3% in 2019, 8.5% in 2020, and 9.7% in 2021) (Figure 4).



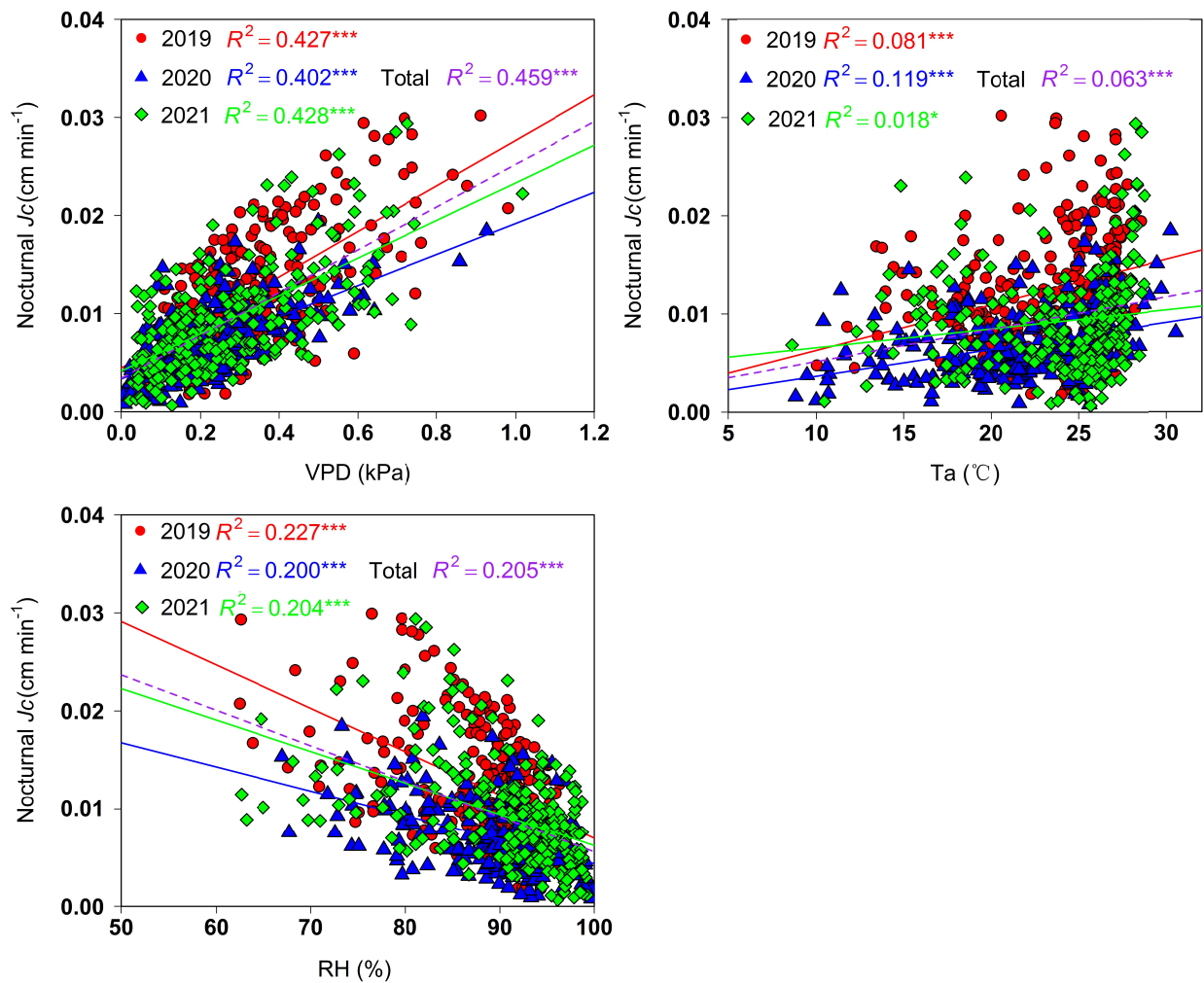
329 **Figure 4.** Annual variation in daily water use (Q_{daily}), daytime water use (Q_{day}), nocturnal water
 330 use (Q_{night}), the ratio of nocturnal to daily water use ($R_{night}=Q_{night}/Q_{daily}$) in 2019, 2020 and 2021,
 331 with some data missing for 2019 due to power supply issues. DOY is day of year.

332 3.3 Factors affecting Tn and predictive modelling

333 Significant and positive linear correlations ($P<0.001$) were found between nocturnal J_C and VPD
 334 ($R^2=0.427$ in 2019, 0.402 in 2020, and 0.428 in 2021) (Figure 5a), with an overall fit R^2 of 0.459
 335 for all data in 3 years. Nocturnal J_C was significant and positively related to Ta ($R^2=0.081$ in
 336 2019, 0.119 in 2020, 0.018 in 2021, and 0.063 for all data in 3 years) (Figure 5b). There was a
 337 significant and negative linear correlation ($P<0.001$) between nocturnal J_C and RH ($R^2=0.227$ in
 338 2019, 0.200 in 2020, 0.204 in 2021, and 0.205 for all data in three years) (Figure 5c). No
 339 significant correlation was found between nocturnal J_C and SWC and WS in *E. urophylla* × *E.*
 340 *grandis* plantation over the 3-year study period.

341 The above analyses found that environmental factors had a low interpretation of nocturnal J_C ,
 342 which is mainly due to the fact that nocturnal J_C is not only caused by Tn, but also by Re. To
 343 develop a highly explanatory model for predicting Tn, we screened all nocturnal J_C and
 344 corresponding VPD, Ta, RH data during the nocturnal stem water saturation period in each year
 345 based on daily diameter variation to reduce the confounding effect of Re (see 2.5 in Materials
 346 and methods). A new dataset was created by randomly selecting a portion of the screened data
 347 from each year, which was used to fit a multiple regression model (i.e., the Tn prediction model),
 348 and the remaining portion of the data from each year was used to validate the model. Regression
 349 analysis showed that excluding Re significantly improved the explanation of the nocturnal J_C fit
 350 of VPD, Ta and RH, increasing the explanations to 80.54%, 39.88% and 42.41%, respectively
 351 (Table 3). Furthermore, compared to the regression model of VPD and Tn, the introduction of Ta
 352 and RH (where RH was rejected) in the multiple regression increased the explained variance by
 353 only 1.3%. When the interaction between VPD, Ta and RH is then introduced (only RH·VPD
 354 was incorporated), the variance explained by the multiple regression can be increased to 82.65%,
 355 an increase of 2.11% over VPD alone (Table 3). In such a case, VPD could be considered as the
 356 main driver of Tn, with Ta having an independent but weak influence, while Ta and RH more
 357 predominantly affect Tn by influencing VPD.

358 The average T_n for remaining portion of the data in 2019, 2020, and 2021 calculated using the
 359 predictive model 5 in Table 3 was $0.00488 \text{ cm}\cdot\text{min}^{-1}$, $0.00483 \text{ cm}\cdot\text{min}^{-1}$ and $0.00343 \text{ cm}\cdot\text{min}^{-1}$,
 360 which was 102.62%, 94.29%, and 106.72% of their actual measured values, respectively, with a
 361 slight overestimation of the model when the measured T_n was less than $0.005 \text{ cm}\cdot\text{min}^{-1}$ and,
 362 conversely, a slight underestimation (Figure 6). The Nash and Sutcliffe coefficient was 0.868 for
 363 2019, 0.948 for 2020, and 0.915 for 2021. In addition, the slopes of the linear fit between the
 364 measured and predicted sets of values for 2019, 2020 and 2021 were 0.905, 0.864 and 0.807,
 365 respectively, with corresponding R^2 values of 0.866, 0.966 and 0.938, respectively (Figure 6),
 366 indicating excellent agreement between these two sets of values. These results thus provide
 367 ample evidence to support the established model for predicting T_n .



368

369 **Figure 5.** Relationship of between nocturnal sap flow density (J_c) with nocturnal mean vapor
 370 pressure deficit (VPD)(a), nocturnal mean atmospheric temperature (T_a)(b), nocturnal mean

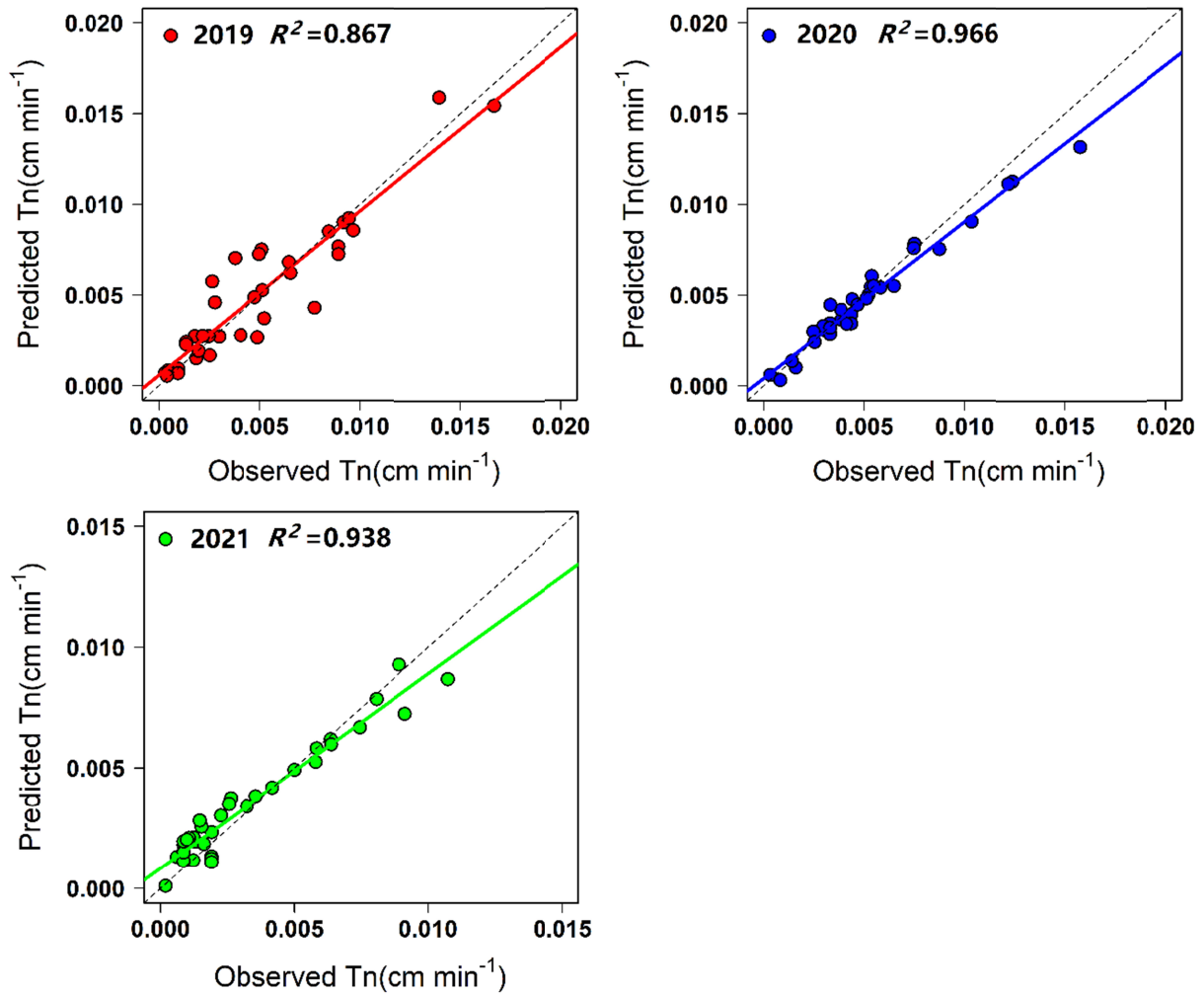
371 relative humidity (RH)(c). The red, blue, and green dots and lines represent the data and
 372 regression lines for 2019, 2020, and 2021, respectively. The purple dashed line is the regression
 373 of all data in 3 years. * represents $P < 0.05$, *** represents $P < 0.001$.

374 **Table 3**

375 *Stepwise Regression Analysis Models of Nocturnal Transpiration Rate (Tn; Nocturnal Sap Flow*
 376 *Density Measured when the Tree Stem Saturated with Water Storage) Versus Vapor Pressure*
 377 *Deficit (VPD), Nocturnal Mean Atmospheric Temperature (Ta) and Nocturnal Mean Relative*
 378 *Humidity (RH).*

Number	Tn prediction model	R^2
1	$T_n = \mathbf{0.0314} \cdot VPD - 0.0048$	0.8054***
2	$T_n = \mathbf{0.00079} \cdot T_a - 0.011$	0.3988***
3	$T_n = \mathbf{-0.00075} \cdot RH + 0.070$	0.4241***
4	$T_n = \mathbf{0.0282} \cdot VPD + \mathbf{0.000185} \cdot T_a - 0.00754$	0.8184***
5	$T_n = \mathbf{0.1148} \cdot VPD + \mathbf{0.000412} \cdot T_a - \mathbf{0.00115} \cdot VPD \cdot RH - 0.00825$	0.8265***

379 **Note:** partial regression slopes in bold are significant ($P < 0.01$), *** represents $P < 0.001$.



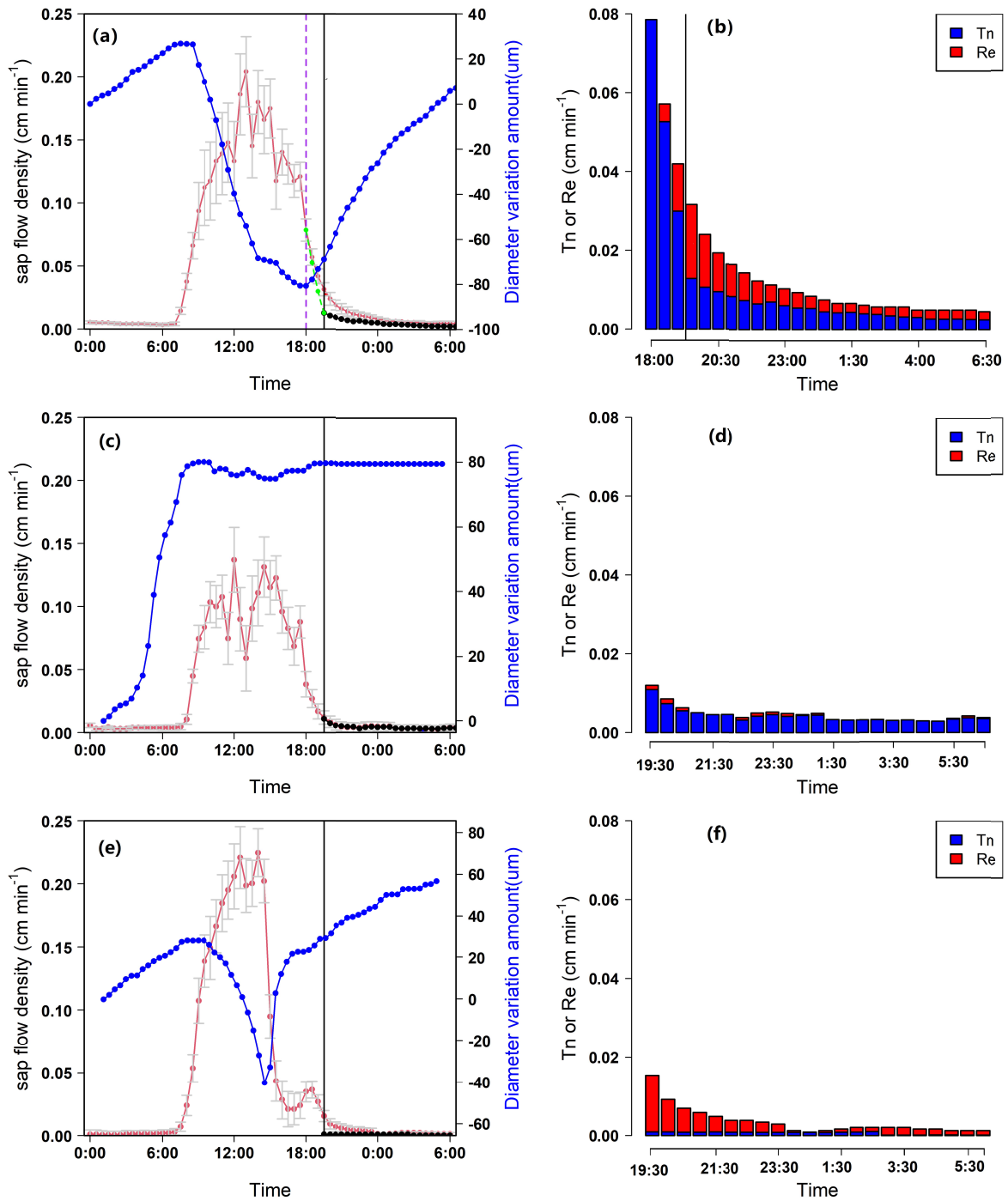
380

381 **Figure 6.** The predicted Tn (cm min⁻¹) plotted against the corresponding observed Tn (J_C during
 382 nocturnal stem saturation period, cm min⁻¹) of *E. urophylla* × *E. grandis* in 2019, 2020 and 2021.
 383 Note: The dotted line denotes the 1:1 relationship, and the solid line indicates the actual
 384 relationship between the predicted and observed values.

385 3.4 Nocturnal J_c components in typical weather conditions

386 The composition of nocturnal J_c varied greatly with weather conditions. When both days and
 387 nights were sunny (e.g., 25-26 August 2021; Fig. 7a-b), nocturnal J_c was related to a
 388 combination of Tn and Re. Re tended to start in the afternoon when transpiration rates decrease
 389 to coincide with root uptake rates, at which time diameter reaches its minimum value for the day
 390 (18: 00 in Figure 7a). As the rate of transpiration continued to decrease, the rate of Re gradually

391 increased, followed by a decreasing stem water deficit due to stem water refilling, resulting in a
392 gradual decrease in the rate of R_e . Thus, the rate of R_e increased and then decreased from the
393 onset of R_e and throughout the night thereafter. Looking only at the night, both R_e and T_n
394 decrease gradually (Figure 7b). During rainy days and sunny nights (e.g., 29-30 August 2021;
395 Figures 7c-d), the stem water deficit was minimal due to the low daytime transpiration and could
396 be rapidly refilled to saturation (Figure 7c). At this time there was essentially no R_e at night and
397 simultaneously sufficient VPD (0.13 kPa-0.24 kPa, mean 0.18 kPa) to drive transpiration, so that
398 the vast majority of the monitored nocturnal J_c was T_n (Figure 7d). This situation also underlies
399 the distinction between T_n and R_e in this study. During sunny days and rainy nights (e.g., 3-4
400 May 2021, Figures 7e-f), the stem water deficit was substantial due to high daytime transpiration
401 (Figure 7e), while at night, due to rainy weather, VPD was minimal and insufficient to drive T_n
402 (0.028 kPa - 0.059 kPa, mean 0.037 kPa), so that all nocturnal J_c during this period was caused
403 by R_e (Figure 7f).



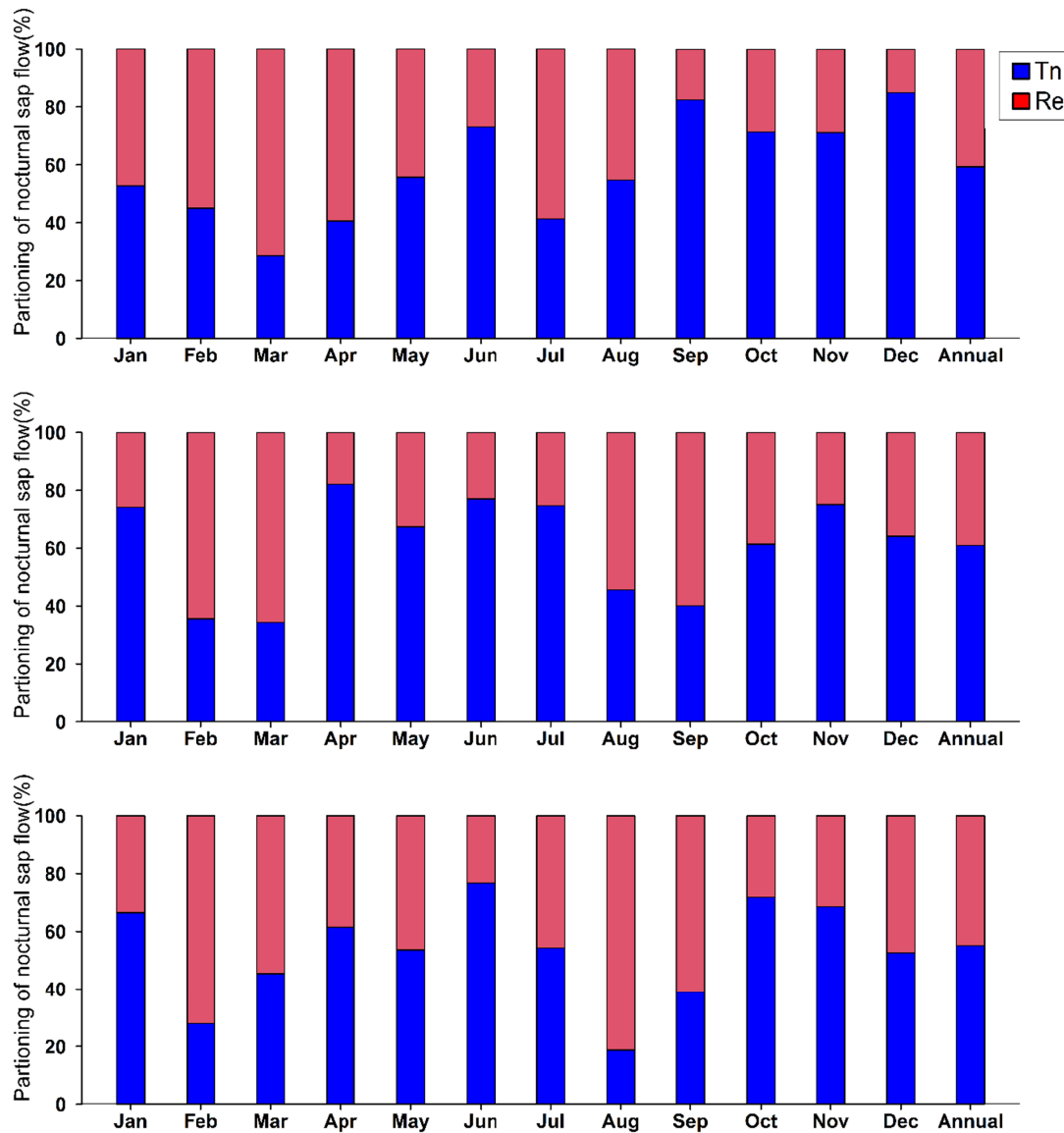
404

405 **Figure 7.** Daily variation of sap flow and tree diameter during sunny days and nights(a), rainy
 406 days and sunny nights(c), sunny days and rainy nights(e). The black vertical line is the boundary
 407 between day and night. The black dots and lines are the model's calculation of Tn variation. The
 408 purple vertical dashed line in (a) is the point at which the diameter begins to increase and

409 nocturnal refilling begins. The green dots and lines in (a) are the actual transpiration rates after
410 estimating the refilling rate from the rate of change in diameter (assuming a linear relationship
411 between the rate of change in diameter and the refilling rate). (b), (d) and (f) are the distribution
412 of transpiration and refilling rates, respectively, corresponding to typical weather conditions on
413 the right (where (b) is drawn from the time when refilling begins and the others from the
414 beginning of the night).

415 **3.5 Contribution of Tn and Re to nocturnal J_c**

416 The contribution of Tn and Re to nocturnal J_c in the *E. urophylla* × *E. grandis* plantation varied
417 considerably among months and even slightly between years (Figure 8). Monthly mean
418 contribution of Tn to nocturnal J_c ranged from 28.6% (March) to 85.1% (December) with an
419 annual mean of 55.28% in 2019, 34.3% (March) to 82.1% (April) with an annual mean of
420 60.29% in 2020, and 18.8% (August) to 76.7% (June) with an annual mean of 61.51% in 2021
421 (Figure 8). Over the 3-year study period, mean contribution of Tn to nocturnal J_c was 58.63%,
422 and the mean contribution of Re to J_c was 41.37%. In addition, the total mean contribution of Re
423 to nocturnal J_c was 43.81% in the dry season and 41.13% in the wet season.



424

425 **Figure 8.** Partitioning of nocturnal sap flow density into nocturnal transpiration and nocturnal
 426 stem refilling in 2019 (top), 2020 (middle) and 2021 (bottom), respectively. Red bars represent
 427 the contribution ratio of stem refilling, blue bars represent the contribution ratio of nocturnal
 428 transpiration.

429 4 Discussion

430 4.1 Daily and nocturnal water use of *E. urophylla* × *E. grandis*

431 During the three years of our investigation, the mean daily transpiration (Q_{daily}) of *E. urophylla* ×
 432 *E. grandis* ranged from 0.98 to 1.49 mm, with annual values ranging from 358.7 to 545.3 mm at

433 stand level. These estimates were comparable to the transpiration recorded in *E. urophylla* × *E.*
434 *grandis* and *E. urophylla* in other regions of China (Morris et al., 2004; Ouyang et al., 2018a;
435 Zhang, 2010) and *E. globulus* in southeastern Australia (Forrester et al., 2010), but was lower
436 than that of *E. urophylla* × *E. grandis* in Brazil (Table S1; 622-879 mm) (Hakamada et al., 2020).
437 The reason for the difference may be a combination of different climatic factors and the higher
438 silvicultural density of *E. globulus* in Brazil (2950 trees ha⁻¹), which resulted in a much higher
439 stand LAI than ours (Table S1). In addition, when compared with other species, *E. urophylla* ×
440 *E. grandis* had a higher transpiration than the 19-year-old *Acacia mangium* (Ma et al., 2008), but
441 not high or even low compared with the transpiration of the 22-year-old Chinese Fir (Ouyang et
442 al., 2018b). It is worth noting that the annual transpiration of *E. urophylla* × *E. grandis* averaged
443 only 33.6% of the annual P during our study period, but due to the uneven distribution of P, this
444 proportion increased to 82.51% during the dry season. When understory transpiration and soil
445 evaporation are added, evapotranspiration from the forest stand during the dry season can be
446 greater than the corresponding P, so the impact of eucalyptus water use on water resources
447 during the dry season should be of particular concern.

448 Nocturnal water use (Q_{night}) is a widespread phenomenon in plants and important for many plant
449 physiological processes (Chen et al., 2020; Chowdhury et al., 2022; Liu et al., 2021; Wu et al.,
450 2020). However, the R_{night} can vary widely among species and different biomes. For example, the
451 value of R_{night} was only 2% and 8% for *red oak* and *red maple* in a mixed New England
452 deciduous forest (Daley & Phillips, 2006), but was 39 % for *Quercus ponderosa* in the
453 Mediterranean region of Prades (Barbeta et al., 2012) and 21% *Pinus ponderosa* in California
454 (Fisher et al., 2007). A study of the nocturnal water use of 98 tree species even found that R_{night}
455 varied from 4.1% to 69% among species (Forster, 2014). In this study, the mean R_{night} of the *E.*
456 *urophylla* × *E. grandis* plantation was 12.66% in 2019, 12.96% in 2020, and 11.43% in 2021,
457 with a 3-year average of 12.35% (Figure 4). This R_{night} is similar to the results of Forster's R_{night}
458 statistics for the phylogenetic group of Eucalyptus (10.27%). Such differences between tree
459 species may be related to their own biology, as nocturnal stomatal conductance is generally
460 higher in deciduous than in evergreen, in broadleaved than in coniferous, and in C4 than in C3
461 plants (Caird et al., 2007; Zeppel et al., 2014). However, there were also two studies found that
462 the R_{night} of different tree species growing in the same area did not differ significantly (Phillips et
463 al., 2010; Zeppel et al., 2010). Zeppel (2013) suggest that this may be the result of a tendency for

464 different plant water uses to show more functional convergence in water-limited areas. From the
465 above, it is clear that the R_{night} of a plant may be influenced by a combination of its own
466 biological characteristics and the environmental conditions.

467 Furthermore, the R_{night} of *E. urophylla* × *E. grandis* showed a clear pattern of seasonal variation,
468 with higher values in dry season than that in wet season (Figure 4). This is consistent with the
469 previous studies of many of the tree species (Di et al., 2019; Forster, 2014; Siddiq & Cao, 2018).
470 Although this may be due to a higher VPD in the dry season than in the wet season (Forster,
471 2014), our results are more likely attributable to an insignificant difference in Q_{night} between the
472 dry and wet seasons, coupled with a significantly lower Q_{daily} in the dry season than in the wet
473 season caused by the combined reduction in atmospheric evaporative demand, available energy
474 (Bosch et al., 2014; Han et al., 2019; Huang et al., 2011), soil moisture content (Lagergren &
475 Lindroth, 2002; Ouyang et al., 2018b; Wang et al., 2019) and LAI (Di et al., 2019; Tie et al.,
476 2017) during the dry season. In wet season, R_{night} was low but still as accounted for 9.5% (3-year
477 average), indicating that Q_{night} is a significant contributor to Q_{daily} . Therefore, Q_{night} should be
478 accurately quantified and taken into account to study the water balance of individual farms,
479 parcels, communities or catchments.

480 **4.2 Environmental drivers of nocturnal J_c**

481 The factors affecting the diurnal J_c and nocturnal J_c of *E. urophylla* × *E. grandis* vary
482 considerably. In one of our previous studies, R_s combined with LAI and SWC were found to be
483 the main factors affecting diurnal transpiration (Wang et al., 2022). However, our observations
484 confirm that VPD is the main factor positively influencing nocturnal J_c in *E. urophylla* × *E.*
485 *grandis*. This may be explained by the fact that VPD can significantly influence the difference in
486 water potential between the leaves and the atmosphere, which contributes to T_n (Zhao et al.,
487 2019). This is also indirect evidence for the existence of T_n in *E. urophylla* × *E. grandis*.
488 Furthermore, the nocturnal J_c of *E. urophylla* × *E. grandis* also showed a close relationship with
489 T_a and RH (Figure 5b, c). However, there was a little improvement in the interpretation of T_n
490 by the multiple regression model when adding T_a , RH and their interactions, compared to VPD
491 alone. Thus, the effects of T_a and RH on nocturnal J_c are also largely mediated by changes in
492 VPD. T_a also had a weak independent effect on T_n (Table 2), which may be related to the fact
493 that increased T_a increases the activity of enzymes involved in transpiration-related

494 physiological processes (Chen et al., 2020). Some previous studies conducted in other forest
495 ecosystems found that the combination of WS and VPD can better explain the nocturnal J_c
496 (Benyon, 1999; Buckley et al., 2011; Daley & Phillips, 2006; Green et al., 1989; Wu et al.,
497 2020). The theory supporting this conclusion is that increased WS may reduce aerodynamic drag
498 and accelerate the diffusion of water vapor through the cuticle and open stomata from moist
499 canopy air to dry overhead air, thus physically increasing nocturnal water loss (Chen et al., 2020;
500 Fisher et al., 2007; Meinzer et al., 1995; Zhao et al., 2015). However, consistent with studies
501 (Fisher et al., 2007; Siddiq & Cao, 2018; Zeppel et al., 2010), our study showed that nocturnal J_c
502 was independent of WS. There is currently no consistent understanding of how increased WS
503 affects nocturnal water loss (Buckley et al., 2011; Campbell-Clause, 1998; Gutierrez et al., 1994).
504 However, the results of this study may be due to the high nocturnal RH of the air at this study
505 site (Figure 3). Although the increase in WS accelerated canopy and upper canopy air exchange,
506 the improvement in canopy air RH was extremely limited. Previous studies suggest that SWC is
507 also an important factor affecting nocturnal water use (Di et al., 2022; Phillips et al., 2010;
508 Zeppel et al., 2010; Zhao et al., 2017), as it not only affects nocturnal stomatal opening and
509 closing through changes in hydraulic conductivity (Cavender-Bares et al., 2007; Zeppel et al.,
510 2012), which in turn affects T_n , but is also a direct source of nocturnal stem R_e (Chen et al.,
511 2020; Wu et al., 2020). Contrary to these studies, no statistically significant correlation between
512 nocturnal J_c and SWC was found in our study. This may be because the soil water supply at the
513 present study site did not reach the stress threshold required to limit the nocturnal sap flow. SWC
514 restrictions on nocturnal water use may be more pronounced in arid and semi-arid ecosystems
515 (Di et al., 2022).

516 **4.3 The method to separate T_n and R_e**

517 The limited interpretation of environmental factors affecting nocturnal J_c (Figure 5) and the
518 reversible increase in nocturnal diameter (Figure 7a) indicated that the nocturnal J_c of *E.*
519 *urophylla* × *E. grandis* was the cause of not only T_n but also R_e (Dietrich et al., 2018; Siddiq &
520 Cao, 2018; Tian et al., 2019). Separating these two components is the key for improving the
521 accuracy of stand water loss estimation and providing a strong foundation for further studies on
522 the mechanistic control over crown nocturnal water use (Phillips et al., 2010). Siddiq & Cao
523 (2018) separated T_n from R_e using the difference in nocturnal sap flow between two special days

524 with similar high daytime VPD and PAR but completely contrasting nocturnal VPD. However,
525 this method can only distinguish nocturnal sap flow on individual days. Limited by the fact that
526 Re varies with daytime transpiration status, the ratio of Tn to Re varied considerably between
527 days, so the representativeness of the conclusions from this method still needs to be verified.
528 Zeppel et al. (2010) have differentiated nocturnal sap flow by simultaneously measuring crown
529 and basal sap flow. This method is relatively accurate, but the technique of installing probes in
530 branches or below the main crown is difficult (which is not feasible for many trees) and costly.
531 Fisher et al. (2007) first proposed three concepts for distinguishing between Tn and Re (Time-
532 separation, back-extrapolation and forecasted refilling, respectively), which have been applied in
533 many studies (Di et al., 2019, 2022). However, Fisher et al. (2007) also found that the results of
534 the three methods varied considerably, with the forecasted refilling method estimated a greater
535 proportion of Re than the time-separation method, while the back-extrapolation method
536 estimated a smaller proportion of Re than the time-separation method. Karpul & West (2016)
537 argued that the time-separation and back-extrapolation methods overestimate and underestimate
538 the actual nocturnal sap flow used for Re , respectively, and that the average of the estimates from
539 the two methods can be used as a more reliable estimate of Re . Our method integrates the
540 advantages of several of these methods, not only circumventing the technical difficulty and cost
541 of installing probes in branches or below the main crown, but also allowing the inference of Tn
542 and Re at any given time, unaffected by daily variations in Re , and with easy access to the
543 relevant parameters. In addition, comparing and verifying with the splitting results of the
544 previous three methods, the Re obtained by our method, although smaller than the time-
545 separation method and larger than the back-extrapolation method, is similar to the average value
546 of the two (Table S2), so we believe that our method can be more reasonable to split the
547 nocturnal water use into Re and Tn , and is worthy of further research and application.

548 The core of our method was to establish a best-fitted Tn prediction model by eliminating the
549 interference from Re on the relationship between Tn and its driving factors, and the difficulty lies
550 in how to remove the interference of Re . The only requirement of our method is to make highly
551 accurate observations of the daily variation in the diameter of the sap flow monitoring sample
552 trees. This is because it is difficult to directly observe the status of Re , but many previous studies
553 have proved that the short-term change in diameter was shown to be proportional related to
554 changes in the volume of water within the stem tissues (Schepper & Steppe, 2010; Zweifel &

555 Häsler, 2001; Zweifel et al., 2001), and this conclusion is supported by the significant positive
556 correlation between our final R_e and the corresponding nocturnal increase in diameter (Figure
557 S2). Thus, the observation of the nocturnal variations in diameter provides the ability to
558 indirectly understand the real-time status of R_e . Under normal circumstances, the diameter of *E.*
559 *urophylla* × *E. grandis* trees increased continuously at night (Figure 7a), indicating that the R_e
560 persisted throughout the night (Dietrich et al., 2018; Vilas et al., 2019; Roman Zweifel, 2016).
561 However, there may still be some special cases in which rainy weather during the day results in
562 R_e being non-existent, or extremely weak but can filling to saturate it quickly (the diameter
563 reaches a short-term maximum and remains constant, as shown in Figure 2 and Figure 7c), while
564 considerable VPD exists at night, in which case the nocturnal J_C monitored is considered to be
565 entirely for T_n (Figure 7c, d). These data were screened to create predictive models of T_n with
566 the corresponding factors (Table 2). The predictive model improved the explanation of T_n to
567 82.65% after excluding the effect of R_e , and good agreement between the predicted and
568 measured values of T_n under the model were also verified (Figure 6), which proved the
569 reliability of the model in predicting T_n . Nevertheless, 17.35% of T_n remained unexplained,
570 which may be due to the fact that T_n is also subject to the regulatory effects of some as yet
571 unidentified intrinsic physiological processes (Chen et al., 2020). Generally, however, our
572 method's results in splitting T_n and R_e are satisfactory. In addition, the concept and framework
573 of our method can be also used as a reference for predicting T_n for other tree species and
574 vegetation types in different regions, and only needs to be optimized for differences in the
575 drivers of T_n for different tree species in different regions (Chen et al., 2020; Wu et al., 2020).
576 For example, in arid and semi-arid regions the effects of SWC may need to be incorporated into
577 the T_n prediction model (Di et al., 2022), whereas for *Acer truncatum* and *Pinus tabuliformis* in
578 Beijing, WS may need to be included in the T_n prediction model (Chen et al., 2020; Wu et al.,
579 2020).

580 4.4 Contribution of T_n and R_e in the nocturnal J_C

581 This study confirmed that the contribution of T_n and R_e to nocturnal J_C varied considerably both
582 across weather conditions and months (Figures 7, 8). This is mainly due to the fact that the both
583 daytime and nighttime environmental factors can vary considerably from day to day. Unlike T_n ,
584 which was mainly affected by nocturnal environmental factors (VPD, T_a and RH; Figure 5), R_e

585 was influenced by the intensity of daytime transpiration. Because main driving force of R_e is the
586 stem water deficit caused by daytime transpiration (Di et al., 2019; Forster, 2014; Siddiq & Cao,
587 2018; Zeppel et al., 2010), any factor affecting daytime and nocturnal transpiration intensity can
588 result in large changes in the ratio of T_n and R_e composition. This also implies that it is
589 unreliable to use the ratio of R_e and T_n for only a few specific days to represent the nocturnal
590 water use components of a stand.

591 The main components of the nocturnal J_C may differ among tree species (Phillips et al., 2010;
592 Siddiq & Cao, 2018; Zeppel et al., 2010). The average ratio of R_e to nocturnal J_C of *E. urophylla*
593 \times *E. grandis* during the 3-year period in this study was 41.37%, which was smaller than the ratio
594 of T_n to nocturnal J_C (58.63%). This result confirmed that the nocturnal J_C observed in the *E.*
595 *urophylla* \times *E. grandis* plantation was mainly used for nocturnal canopy transpiration, which is
596 consistent with the results of the study on two evergreen temperate woodland species (*E.*
597 *parramattensis* and *Angophora bakeri*) (Zeppel et al., 2010) and some broadleaf timber species
598 under a tropical seasonal climate (Siddiq & Cao, 2018), but contrasts with the results of the study
599 on a mature poplar plantation (Di et al., 2022) and *Acer truncatum* (Wu et al., 2020).

600 There were no differences between the dry and wet seasons in the ratio of R_e in the *E. urophylla*
601 \times *E. grandis* plantation. This result rejects our initial conjecture that the ratio of R_e would be
602 higher in the dry season compared to the wet season. Some studies considered that the capacitive
603 discharge of stored water in the stem could reduce the risk of xylem embolism and hydraulic
604 failure (Bucci et al., 2004; McDonald et al., 2002; Phillips et al., 2003; Yi et al., 2017). It could
605 also increase the water potential of stems and leaves before dawn to induce stomatal conductance
606 (Percy, 1988). This can increase the duration of photosynthesis and alleviate the carbon fixation
607 process of plants affected by drought stress (Yu et al., 2016). Thus, the phenomenon of
608 increasing the ratio of R_e in plants under drought stress has been identified in some studies and is
609 considered to be a survival strategy for plants to survive drought (Berbigier et al., 1996).
610 However, in a study of soil moisture dependent nocturnal water use strategy in a mature poplar
611 plantation (Di et al., 2022), there was an opposite variation in the ratio of R_e with soil moisture
612 input, demonstrating that poplars are instead more dependent on stem water storage to sustain
613 rapid diurnal transpiration under wetter soil conditions. The conflicting results may be due to the
614 differences in the biological characteristics among tree species. In this study, the ratio of R_e in *E.*

615 *urophylla* × *E. grandis* was greater in some months of dry seasons than in wet seasons, but there
616 were also some months with opposite results (Figure 8), with no significant differences on
617 average overall. Such results may indicate that physiological processes such as diurnal
618 transpiration in the *E. urophylla* × *E. grandis* plantation may not be highly dependent on stem
619 water storage under the soil moisture conditions of this study area.

620 **5 Conclusions**

621 Our results from a 3-year study in *E. urophylla* × *E. grandis* plantations in southern China
622 indicated that annual transpiration ranged from 358.7 mm to 545.3 mm, accounting for 33.6% of
623 annual rainfall. However, the transpiration during the dry season accounted for 82.5% of the
624 corresponding rainfall, implying the effects of water use in dry season on regional water security
625 of eucalyptus in China deserves special attention. In addition, there was also substantial
626 nocturnal water use in the *E. urophylla* × *E. grandis* plantation in south China, accounting for an
627 average of approximately 12.35% of Q_{daily} , and this proportion would increase significantly
628 during the dry season. This implies that nocturnal water use should not be neglected in a
629 multiscale vegetation water balance model. Nocturnal water use of *E. urophylla* × *E. grandis* is
630 used for both Tn and Re, and Tn is influenced by a combination of nocturnal VPD, Ta and RH,
631 with VPD being the dominant driver. Based on the relationship between daily variation in
632 diameter and stem water storage, we have developed a new method to separated Re from Tn. The
633 results of the separation showed that the proportion of Re varied considerably across weather and
634 months. In this study, the 3-year mean of the ratio of Re for *E. urophylla* × *E. grandis* was
635 41.37%, which was significant smaller than the value of Tn, indicating that the nocturnal water
636 use in *E. urophylla* × *E. grandis* is mainly used Tn (58.63%) rather than Re. The lack of
637 variation in Re ratios between the dry and wet seasons also suggests a low dependence on stem
638 water storage during the dry season for *E. urophylla* × *E. grandis* in this study area. Our results
639 can help to properly understand the processes of nocturnal water use and its control mechanisms,
640 and can also provide a reference for further refinement of multiscale water balance models for *E.*
641 *urophylla* × *E. grandis*.

642 **Acknowledgments**

643 This study was financially supported by the Natural Science Foundation of Guangdong Province
644 (2021A1515010560); Forestry Science and Technology Innovation Project of Guangdong
645 Province (2018KJCX014); Guangdong Forestry Ecological Monitoring Network Platform
646 Construction Project (2021CG535) and the Operation Project for Guangdong Zhanjiang
647 Eucalyptus Forest Ecosystem National Positioning Observation and Research Station. We thank
648 the assistance of the staffs from South China Experiment Nursery for support during the
649 selection of suitable plots of this study.

650 **Conflict of Interest**

651 The authors declare that they have no known competing financial interests or personal
652 relationships that could have appeared to influence the work reported in this paper.

653 **Data Availability Statement**

654 Data on the physico-chemical properties of the soil and information on the sample trees at the
655 test site are given in Tables 1 and 2, respectively. Other analytical data are available at Figshare
656 repository via (Wang et al., 2023) <https://doi.org/10.6084/m9.figshare.24076899.v1> with CC-BY
657 4.0.

658 **References**

- 659 Arnold, R., Xie, Y., Luo, J., Wang, H., & Midgley, S. (2020). A tale of two genera: exotic Eucalyptus and
660 Acacia species in China. 1. Domestication and research. *International Forestry Review*, 22(1), 1-18.
661 <https://doi.org/10.1505/146554820829403441>
- 662 Barbeta, A., Ogaya, R., & Peñuelas, J. (2012). Comparative study of diurnal and nocturnal sap flow of
663 *Quercus ilex* and *Phillyrea latifolia* in a Mediterranean holm oak forest in Prades (Catalonia, NE Spain).
664 *Trees*, 26(5), 1651-1659. <https://doi.org/10.1007/s00468-012-0741-4>
- 665 Benyon, R. G. (1999). Nighttime water use in an irrigated *Eucalyptus grandis* plantation. *Tree Physiology*,
666 19(13), 853-859. <https://doi.org/10.1093/treephys/19.13.853>
- 667 Berbigier, P., Bonnefond, J. M., Loustau, D., Ferreira, M. I., David, J. S., & Pereira, J. S. (1996). Transpiration
668 of a 64-year-old maritime pine stand in Portugal. *Oecologia*, 107, 43-52.
669 <https://doi.org/10.1007/BF00582233>

- 670 Bosch, D. D., Marshall, L. K., & Teskey, R. (2014). Forest transpiration from sap flux density measurements
671 in a Southeastern Coastal Plain riparian buffer system - ScienceDirect. *Agricultural and Forest*
672 *Meteorology*, 187(8), 72-82. <https://doi.org/10.1016/j.agrformet.2013.12.002>
- 673 Bucci, S. J., Scholz, F. G., Goldstein, G., Meinzer, F. C., Hinojosa, J. A., Hoffmann, W. A., & Franco, A. C.
674 (2004). Processes preventing nocturnal equilibration between leaf and soil water potential in tropical
675 savanna woody species. *Tree Physiology*, 24(10), 1119-1127. <https://doi.org/10.1093/treephys/24.10.1119>
- 676 Buckley, T. N., Turnbull, T. L., Pfautsch, S., & Adams, M. A. (2011). Nocturnal water loss in mature
677 subalpine *Eucalyptus delegatensis* tall open forests and adjacent *E. pauciflora* woodlands. *Ecology and*
678 *Evolution*, 1(3), 435-450. <https://doi.org/10.1002/ece3.44>
- 679 Caird, M. A., Richards, J. H., & Donovan, L. A. (2007). Nighttime stomatal conductance and transpiration in
680 C3 and C4 plants. *Plant Physiology*, 143(1), 4-10. <https://doi.org/10.1104/pp.106.092940>
- 681 Campbell-Clause, J. M. (1998). Stomatal response of grapevines to wind. *Australian Journal of Experimental*
682 *Agriculture*, 38(1), 77-82. <https://doi.org/10.1071/EA91220>
- 683 Campbell, G. S., & Norman, J. (1998). *An introduction to environmental biophysics* (second ed.). New York,
684 NY, USA: Springer.
- 685 Cavender-Bares, J., Sack, L., & Savage, J. (2007). Atmospheric and soil drought reduce nocturnal conductance
686 in live oaks. *Tree Physiology*, 27(4), 611-620. <https://doi.org/10.1093/treephys/27.4.611>
- 687 Chan, T., Hölttä, T., Berninger, F., Mäkinen, H., Nöjd, P., Mencuccini, M., & Nikinmaa, E. (2016). Separating
688 water-potential induced swelling and shrinking from measured radial stem variations reveals a cambial
689 growth and osmotic concentration signal. *Plant Cell and Environment*, 39, 233-244.
690 <https://doi.org/10.1111/pce.12541>
- 691 Chen, Z., Zhang, Z., Sun, G., Chen, L., Xu, H., & Chen, S. (2020). Biophysical controls on nocturnal sap flow
692 in plantation forests in a semi-arid region of northern China. *Agricultural and Forest Meteorology*, 284,
693 107904. <https://doi.org/10.1016/j.agrformet.2020.107904>
- 694 Chowdhury, F. I., Arteaga, C., Alam, M. S., Alam, I., & Dios, V. R. d. (2022). Drivers of nocturnal stomatal
695 conductance in C3 and C4 plants. *Science of the Total Environment*, 814, 151952.
696 <https://doi.org/10.1016/j.scitotenv.2021.151952>
- 697 Claudia, C., Giovanni, M., Alessio, G., Claudio, C., Mauro, C., & Roberto, T. (2015). Simultaneous
698 measurements of stem radius variation and sap flux density reveal synchronisation of water storage and
699 transpiration dynamics in olive trees. *Ecohydrology*, 8, 33-45. <https://doi.org/10.1002/eco.1483>
- 700 Corell, M., Martín-Palomo, M. J., Girón, I., Andreu, L., Trigo, E., López-Moreno, Y. E., et al. (2019).
701 Approach using trunk growth rate data to identify water stress conditions in olive trees. *Agricultural Water*
702 *Management*, 222, 12-20. <https://doi.org/10.1016/j.agwat.2019.05.029>.
- 703 Daley, M. J., & Phillips, N. G. (2006). Interspecific variation in nighttime transpiration and stomatal
704 conductance in a mixed New England deciduous forest. *Tree Physiology*, 26(4), 411-419.
705 <https://doi.org/10.1093/treephys/26.4.411>

- 706 Di, N., Xi, B., Clothier, B., Wang, Y., Li, G., & Jia, L. (2019). Diurnal and nocturnal transpiration behaviors
707 and their responses to groundwater-table fluctuations and meteorological factors of *Populus tomentosa* in
708 the North China Plain. *Forest Ecology and Management*, 448, 445-456.
709 <https://doi.org/10.1016/j.foreco.2019.06.009>
- 710 Di, N., Yang, S., Liu, Y., Fan, Y., Duan, J., Nadezhdina, N., et al. (2022). Soil-moisture-dependent nocturnal
711 water use strategy and its responses to meteorological factors in a seasonal-arid poplar plantation.
712 *Agricultural Water Management*, 274, 107984. <https://doi.org/10.1016/j.agwat.2022.107984>
- 713 Dietrich, L., Zweifel, R., & Kahmen, A. (2018). Daily stem diameter variations can predict the canopy water
714 status of mature temperate trees. *Tree Physiology*, 38(7), 941-952. <https://doi.org/10.1093/treephys/tpy023>
- 715 Doronila, A. I., & Forster, M. A. (2015). Performance Measurement Via Sap Flow Monitoring of Three
716 Eucalyptus Species for Mine Site and Dryland Salinity Phytoremediation. *International Journal of*
717 *Phytoremediation*, 17(2), 101-108. <https://doi.org/10.1080/15226514.2013.850466>
- 718 Engel, V., Jobbágy, E. G., Stieglitz, M., Williams, M., & Jackson, R. B. (2005). Hydrological consequences of
719 Eucalyptus afforestation in the Argentine Pampas. *Water Resources Research*, 41(10), 3053-3057.
720 <https://doi.org/10.1029/2004WR003761>
- 721 Escalona, J. M., Fuentes, S., Tomás, M., Martorell, S., Flexas, J., & Medrano, H. (2013). Responses of leaf
722 night transpiration to drought stress in *Vitis vinifera* L. *Agricultural Water Management*, 118, 50-58.
723 <https://doi.org/10.1016/j.agwat.2012.11.018>
- 724 Fang, W., Lv, N., & Fu, B. (2018). Research advances in nighttime sap flow density, its physiological
725 implications, and influencing factors in plants. *Acta Ecologica Sinica*, 38(21), 4-12.
726 <https://doi.org/10.5846/stxb201802080337>
- 727 Fisher, J. B., Baldocchi, D. D., Misson, L., Dawson, T. E., & Goldstein, A. H. (2007). What the towers don't
728 see at night: Nocturnal sap flow in trees and shrubs at two AmeriFlux sites in California. *Tree Physiology*,
729 27(4), 597-610. <https://doi.org/10.1093/treephys/27.4.597>
- 730 Forrester, D. I., Collopy, J. J., & Morris, J. D. (2010). Transpiration along an age series of *Eucalyptus globulus*
731 plantations in southeastern Australia. *Forest Ecology and Management*, 259(9), 1754-1760.
732 <https://doi.org/10.1016/j.foreco.2009.04.023>.
- 733 Forster, M. A. (2014). How significant is nocturnal sap flow? *Tree Physiology*, 34(7), 757-765.
734 <https://doi.org/10.1093/treephys/tpu051>
- 735 Granier, A. (1987). Evaluation of transpiration in a Douglas-fir stand by means of sap flow measurements.
736 *Tree Physiology*, 3(4), 309-320. <https://doi.org/10.1093/treephys/3.4.309>
- 737 Green, S. R., McNaughton, K. G., & B.E Clothier. (1989). Observations of night-time water use in kiwifruit
738 vines and apple trees. *Agricultural and Forest Meteorology*, 48(3), 251-261. [https://doi.org/10.1016/0168-](https://doi.org/10.1016/0168-1923(89)90072-5)
739 [1923\(89\)90072-5](https://doi.org/10.1016/0168-1923(89)90072-5)

- 740 Gutierrez, M. V., Meinzer, F. C., & Grantz, D. A. (1994). Regulation of transpiration in coffee hedgerows:
741 covariation of environmental variables and apparent responses of stomata to wind and humidity. *Plant Cell
742 and Environment*, 17(12), 1305–1313. <https://doi.org/10.1111/j.1365-3040.1994.tb00532.x>
- 743 Hakamada, R. E., Hubbard, R. M., Moreira, G. G., Stape, J. L., Campoe, O., & de Barros Ferraz, S. F. (2020).
744 Influence of stand density on growth and water use efficiency in Eucalyptus clones. *Forest Ecology and
745 Management*, 466, 118125. <https://doi.org/10.1016/j.foreco.2020.118125>
- 746 Han, C., Chen, N., Zhang, C., Liu, Y., Khan, S., Lu, K., et al. (2019). Sap flow and responses to
747 meteorological about the Larix principis-rupprechtii plantation in Gansu Xinlong Mountain, northwestern
748 China. *Forest Ecology and Management*, 451, 117519. <https://doi.org/10.1016/j.foreco.2019.117519>
- 749 Hasholt, B. (1997). *Distributed hydrological modelling: applications of the topmodel concept*. Chichester,
750 U.K: Wiley.
- 751 Herzog, K. M., Häslér, R., & Thum, R. (1995). Diurnal changes in the radius of a subalpine Norway spruce
752 stem: their relation to the sap flow and their use to estimate transpiration. *Trees*, 10, 94-
753 101. <https://doi.org/10.1007/BF00192189>
- 754 Huang, Y., Li, X., Zhang, Z., He, C., Zhao, P., You, Y., & Mo, L. (2011). Seasonal changes in
755 Cyclobalanopsis glauca transpiration and canopy stomatal conductance and their dependence on
756 subterranean water and climatic factors in rocky karst terrain. *Journal of Hydrology*, 402(1-2), 135-143.
757 <https://doi.org/10.1016/j.jhydrol.2011.03.013>
- 758 IUSS Working Group WRB. (2006). *World reference base for soil resource 2006 in: World Soil Resources
759 Reports no. 103, 2nd ed.* Rome: FAO.
- 760 Jarvis, P. G. (1976). The Interpretation of the Variations in Leaf Water Potential and Stomatal Conductance
761 Found in Canopies in the Field. *Philosophical Transactions of the Royal Society of London*, 273(927), 593-
762 610. <https://doi.org/10.1098/rstb.1976.0035>
- 763 Jiménez, M. N., Navarro, F. B., Sánchez-Miranda, A., & Ripoll, M. A. (2019). Using stem diameter variations
764 to detect and quantify growth and relationships with climatic variables on a gradient of thinned Aleppo
765 pines. *Forest Ecology and Management*, 442, 53-62. <https://doi.org/10.1016/j.foreco.2019.03.061>
- 766 Jonard, F., André, F., Ponette, Q., Vincke, C., & Jonard, M. (2011). Sap flux density and stomatal conductance
767 of European beech and common oak trees in pure and mixed stands during the summer drought of 2003.
768 *Journal of Hydrology*, 409(1-2), 371-381. <https://doi.org/10.1016/j.jhydrol.2011.08.032>
- 769 Karpul, R. H., & West, A. G. (2016). Wind drives nocturnal, but not diurnal, transpiration in
770 Leucospermum conocarpodendron trees: Implications for stiling on the Cape Peninsula. *Tree Physiology*,
771 36(8), 954-966. <https://doi.org/10.1093/treephys/tpw033>
- 772 Kropp, H., Loranty, M., Alexander, H. D., Berner, L. T., Natali, S. M., & Spawn, S. A. (2017). Environmental
773 constraints on transpiration and stomatal conductance in a Siberian Arctic boreal forest. *Journal of
774 Geophysical Research: Biogeosciences*, 122(3), 487-497. <https://doi.org/10.1002/2016JG003709>

- 775 Kumagai, T. o., Aoki, S., Nagasawa, H., Mabuchi, T., Kubota, K., Inoue, S., et al. (2005). Effects of tree-to-
776 tree and radial variations on sap flow estimates of transpiration in Japanese cedar. *Agricultural and Forest*
777 *Meteorology*, 135(1-4), 110-116. <https://doi.org/10.1016/j.agrformet.2005.11.007>
- 778 Lagergren, F., & Lindroth, A. (2002). Transpiration response to soil moisture in pine and spruce trees in
779 Sweden. *Agricultural and Forest Meteorology*, 112(2), 67-85. [https://doi.org/10.1016/S0168-
780 1923\(02\)00060-6](https://doi.org/10.1016/S0168-1923(02)00060-6)
- 781 Liu, W., Wu, J., Fan, H., Duan, H., Li, Q., Yuan, Y., & Zhang, H. (2017). Estimations of evapotranspiration in
782 an age sequence of Eucalyptus plantations in subtropical China. *Plos One*, 12(4), e0174208.
783 <https://doi.org/10.1371/journal.pone.0174208>
- 784 Liu, Z., Liu, Q., Wei, Z., Yu, X., Jia, G., & Jiang, J. (2021). Partitioning tree water usage into storage and
785 transpiration in a mixed forest. *Forest Ecosystems*, 8(72). <https://doi.org/10.1186/s40663-021-00353-5>
- 786 Lu, P., Urban, L., & Zhao, P. (2004). Granier's Thermal Dissipation Probe (TDP) Method for Measuring Sap
787 Flow in Trees: Theory and Practice. *Acta Botanica Sinica* 46(6), 631-646.
788 <https://doi.org/10.3321/j.issn:1672-9072.2004.06.001>
- 789 Ma, L., Lu, P., Zhao, P., Rao, X., Cai, X., & Zeng, X. (2008). Diurnal, daily, seasonal and annual patterns of
790 sap-flux-scaled transpiration from an Acacia mangium plantation in South China. *Annals of Forest Science*,
791 65, 402.<https://doi.org/10.1051/forest:2008013>
- 792 Marks, C. O., & Lechowicz, M. J. (2007). The ecological and functional correlates of nocturnal transpiration.
793 *Tree Physiology*, 27(4), 577-584. <https://doi.org/10.1093/treephys/27.4.577>
- 794 Mcdonald, E. P., Erickson, J. E., & Kruger, E. L. (2002). Research note: Can decreased transpiration limit
795 plant nitrogen acquisition in elevated CO₂? *Functional Plant Biology*, 29(9), 1115-1120.
796 <https://doi.org/10.1071/FP02007>
- 797 Meidner, H., & Mansfield, T. A. (1965). Stomatal responses to illumination. *Biological Reviews*, 40(4), 483-
798 508. <https://doi.org/10.1111/j.1469-185X.1965.tb00813.x>
- 799 Meinzer, F. C., Goldstein, G., Jackson, P., Holbrook, N. M., Guti6rrez, M. V., & Cavelier, J. (1995).
800 Environmental and physiological regulation of transpiration in tropical forest gap species: the influence of
801 boundary layer and hydraulic properties *Oecologia*, 101, 514-522. <https://doi.org/10.1007/BF00329432>
- 802 Morris, J., Ningnan, Z., Zengjiang, Y., Collopy, J., & Daping, X. (2004). Water use by fast-growing Eucalyptus
803 urophylla plantations in southern China. *Tree Physiology*, 24(9), 1035-
804 1044.<https://doi.org/10.1093/treephys/24.9.1035>
- 805 Ouyang, L., Zhao, P., Zhou, G., Zhu, L., Huang, Y., Zhao, X., & Ni, G. (2018a). Stand - scale transpiration of
806 a *Eucalyptus urophylla* × *Eucalyptus grandis* plantation and its potential hydrological implication.
807 *Ecohydrology*, 11(4), e1938.<https://doi.org/10.1002/eco.1938>

- 808 Ouyang, S., Xiao, K., Zhao, Z., Xiang, W., Xu, C., Lei, P., et al. (2018b). Stand transpiration estimates from
809 recalibrated parameters for the granier equation in a Chinese Fir (*Cunninghamia lanceolata*) plantation in
810 southern China. *Forests*, 9(4), 162. <https://doi.org/10.3390/f9040162>
- 811 Paul, K., Horna, V., & Leuschner, C. (2012). Environmental control of daily stem growth patterns in five
812 temperate broad-leaved tree species. *Tree Physiology*, 32(8), 1021-1032.
813 <https://doi.org/10.1093/treephys/tps049>
- 814 Pearcy, R. W. (1988). Photosynthetic Utilisation of Lightflecks by Understory Plants. *Australian Journal of*
815 *Plant Physiology*, 15(2), 223-238. <https://doi.org/10.1071/PP9880223>
- 816 Pei, Y., Huang, L., Zhang, Y., & Pan, Y. (2023). Water use pattern and transpiration of Mongolian pine
817 plantations in relation to stand age on northern Loess Plateau of China. *Agricultural and Forest*
818 *Meteorology*, 330, 109320. <https://doi.org/10.1016/j.agrformet.2023.109320>
- 819 Peters, E. B., McFadden, J. P., & Montgomery, R. A. (2010). Biological and environmental controls on tree
820 transpiration in a suburban landscape. *Journal of Geophysical Research: Biogeosciences*,
821 115(G4).<https://doi.org/10.1029/2009JG001266>
- 822 Phillips, N. G., Lewis, J. D., Logan, B. A., & Tissue, D. T. (2010). Inter- and intra-specific variation in
823 nocturnal water transport in Eucalyptus. *Tree Physiology*, 30(5), 586-596.
824 <https://doi.org/10.1093/treephys/tpq009>
- 825 Phillips, N. G., Ryan, M. G., Bond, B. J., McDowell, N. G., Hinckley, T. M., & Čermák, J. (2003). Reliance on
826 stored water increases with tree size in three species in the Pacific Northwest. *Tree Physiology*, 23(4), 237-
827 245. <https://doi.org/10.1093/treephys/23.4.237>
- 828 Priestley, C. H. B., & Taylor, R. J. (1972). On the Assessment of Surface Heat Flux and Evaporation Using
829 Large Scale Parameters. *Monthly Weather Review*, 100(2), 81-92. [https://doi.org/10.1175/1520-0493\(1972\)100<0081:OTAOSH>2.3.CO;2](https://doi.org/10.1175/1520-0493(1972)100<0081:OTAOSH>2.3.CO;2)
- 830
- 831 Ritchie, J. T. (1974). Atmospheric and soil water influences on the plant water balance. *Agricultural*
832 *Meteorology*, 14(1-2), 183-198. [https://doi.org/10.1016/0002-1571\(74\)90018-1](https://doi.org/10.1016/0002-1571(74)90018-1)
- 833 Rosado, B. H. P., Oliveira, R. S., Joly, C. A., Aidar, M. P. M., & Burgess, S. S. O. (2012). Diversity in
834 nighttime transpiration behavior of woody species of the Atlantic Rain Forest, Brazil. *Agricultural and*
835 *Forest Meteorology*, 158, 13-20. <https://doi.org/10.1016/j.agrformet.2012.02.002>
- 836 Schepper, V. D., & Steppe, K. (2010). Development and verification of a water and sugar transport model
837 using measured stem diameter variations. *Journal of Experimental Botany*, 61(8), 2083-2099.
838 <https://doi.org/10.1093/jxb/erq018>
- 839 Sellin, A., & Lubenets, K. (2010). Variation of transpiration within a canopy of silver birch: effect of canopy
840 position and daily versus nightly water loss. *Ecohydrology*, 3(4), 467-477. <https://doi.org/10.1002/eco.133>
- 841 Siddiq, Z., & Cao, K.-F. (2018). Nocturnal transpiration in 18 broadleaf timber species under a tropical
842 seasonal climate. *Forest Ecology and Management*, 418, 47-54. <https://doi.org/10.1016/j.foreco.2017.12.043>

- 843 Snyder, K. A., Richards, J. H., & Donovan, L. A. (2003). Night-time conductance in C3 and C4 species: do
844 plants lose water at night? *Journal of Experimental Botany*, 54(383), 861-865.
845 <https://doi.org/10.1093/jxb/erg082>
- 846 Tian, Y., Zhang, Q., Liu, X., Meng, M., & Wang, B. (2019). The Relationship between Stem Diameter
847 Shrinkage and Tree Bole Moisture Loss Due to Transpiration. *Forests*, 10(3), 290.
848 <https://doi.org/10.3390/f10030290>
- 849 Tie, Q., Hu, H., Tian, F., Guan, H., & Lin, H. (2017). Environmental and physiological controls on sap flow in
850 a subhumid mountainous catchment in North China. *Agricultural and Forest Meteorology*, 240-241, 46-57.
851 <https://doi.org/10.1016/j.agrformet.2017.03.018>
- 852 Vilas, M. P., Adams, M. P., Ball, M. C., Meynecke, J.-O., Santini, N. S., Swales, A., & Lovelock, C. E.
853 (2019). Night and day: Shrinking and swelling of stems of diverse mangrove species growing along
854 environmental gradients. *Plos One*, 14(9), e0221950. <https://doi.org/10.1371/journal.pone.0221950>
- 855 Wang, H., Zhao, P., Cai, X., Wang, Q., Ma, L., Rao, X., & Zeng, X. (2007). Partitioning of night sap flow of
856 *Acacia mangium* and its implication for estimating whole-tree transpiration. *Journal of Plant Ecology*,
857 31(5), 777-786. <https://doi.org/10.17521/cjpe.2007.0099>
- 858 Wang, H., Zhao, P., Hölscher, D., Wang, Q., Lu, P., Cai, X., & Zeng, X. (2012). Nighttime sap flow of *Acacia*
859 *mangium* and its implications for nighttime transpiration and stem water storage. *Journal of Plant Ecology*,
860 5(3), 294-304. <https://doi.org/10.1093/jpe/rtr025>
- 861 Wang, Y., Cao, G., Wang, Y., Webb, A. A., Yu, P., & Wang, X. (2019). Response of the daily transpiration of
862 a larch plantation to variation in potential evaporation, leaf area index and soil moisture. *Scientific Reports*,
863 9, 4697. <https://doi.org/10.1038/s41598-019-41186-1>
- 864 Wang, Z., Liu, S., Xu, Y., Zhu, W., & Du, A. (2022). Differences in Transpiration Characteristics among
865 *Eucalyptus* Plantations of Three Species on the Leizhou Peninsula, Southern China. *Forests*, 13(10), 1544.
866 <https://doi.org/10.3390/f13101544>
- 867 Wu, J., Liu, H., Zhu, J., Gong, L., Xu, L., Jin, G., et al. (2020). Nocturnal sap flow is mainly caused by stem
868 refilling rather than nocturnal transpiration for *Acer truncatum* in urban environment. *Urban Forestry &*
869 *Urban Greening*, 56, 126800. <https://doi.org/10.1016/j.ufug.2020.126800>
- 870 Xu, Y., Du, A., Wang, Z., Zhu, W., Li, C., & Wu, L. (2020). Effects of different rotation periods of *Eucalyptus*
871 plantations on soil physiochemical properties, enzyme activities, microbial biomass and microbial
872 community structure and diversity. *Forest Ecology and Management*, 456, 117683.
873 <https://doi.org/10.1016/j.foreco.2019.117683>
- 874 Xue, F., Jiang, Y., Dong, M., Wang, M., Ding, X., Yang, X., et al. (2022). Different drought responses of stem
875 water relations and radial increments in *Larix principis-rupprechtii* and *Piceameyeri* in a montane mixed
876 forest. *Agricultural and Forest Meteorology*, 315, 108817. <https://doi.org/10.1016/j.agrformet.2022.108817>

- 877 Yi, K., Dragoni, D., Phillips, R. P., Roman, D. T., & Novick, K. A. (2017). Dynamics of stem water uptake
878 among isohydric and anisohydric species experiencing a severe drought. *Tree Physiology*, 37(10), 1379-
879 1392. <https://doi.org/10.1093/treephys/tpw126>
- 880 Yu, T., Feng, Q., Si, J., Mitchell, P. J., Forster, M. A., Zhang, X., & Zhao, C. (2018). Depressed hydraulic
881 redistribution of roots more by stem refilling than by nocturnal transpiration for *Populus euphratica* Oliv. in
882 situ measurement. *Ecology and Evolution*, 8(5), 2607-2616. <https://doi.org/10.1002/ece3.3875>
- 883 Yu, T., Feng, Q., Si, J., Zhang, X., Alec, D., & Zhao, C. (2016). Evidences and magnitude of nighttime
884 transpiration derived from *Populus euphratica* in the extreme arid region of China. *Journal of Plant Biology*,
885 59(6), 648-657. <https://doi.org/10.1007/s12374-015-0536-4>
- 886 Zeppel, M. (2013). Convergence of tree water use and hydraulic architecture in water - limited regions: A
887 review and synthesis. *Ecohydrology*, 6(5), 889-900. <https://doi.org/10.1002/eco.1377>
- 888 Zeppel, M. J. B., Lewis, J. D., Phillips, N. G., & Tissue, D. T. (2014). Consequences of nocturnal water loss: a
889 synthesis of regulating factors and implications for capacitance, embolism and use in models. *Tree*
890 *Physiology*, 34(10), 1047-1055. <https://doi.org/10.1104/pp.106.092940>
- 891 Zeppel, M., Tissue, D., Taylor, D., Macinnis-Ng, C., & Eamus, D. (2010). Rates of nocturnal transpiration in
892 two evergreen temperate woodland species with differing water-use strategies. *Tree Physiology*, 30(8), 988-
893 1000. <https://doi.org/10.1093/treephys/tpq053>
- 894 Zeppel, M. J. B., Lewis, J. D., Chaszar, B., Smith, R. A., Medlyn, B. E., Huxman, T. E., & Tissue, D. T.
895 (2012). Nocturnal stomatal conductance responses to rising [CO₂], temperature and drought. *New*
896 *Phytologist*, 193(4), 929-938. <https://doi.org/10.1111/j.1469-8137.2011.03993.x>
- 897 Zeppel, M. J. B., Lewis, J. D., Medlyn, B., Barton, C. V., Duursma, R. A., Eamus, D., et al. (2011). Interactive
898 effects of elevated CO₂ and drought on nocturnal water fluxes in *Eucalyptus saligna*. *Tree Physiology*,
899 31(9), 932-944. <https://doi.org/10.1093/treephys/tpq024>
- 900 Zhang, N. (2010). Studies on water use of eucalyptus plantations in Guangdong. (Doctor), Chinese Academy
901 of Forestry Beijing.
- 902 Zhao, C., Si, J., Feng, Q., Yu, T., Li, P., & Forster, M. A. (2019). Nighttime transpiration of *Populus*
903 *euphratica* during different phenophases. *Journal of Forestry Research*, 30(2), 435-444.
904 <https://doi.org/10.1007/s11676-018-0672-z>
- 905 Zhao, C., Si, J., Qi, F., Yu, T., & Li, P. (2015). Effect of wind speed on transpiration rate of *Populus euphratica*
906 in extreme arid deserts. *Journal of Glaciology and Geocryology*, 37(4), 1104-1111.
907 <https://doi.org/10.7522/j.issn.1000-0240.2015.0123>
- 908 Zhao, C., Si, J., Qi Feng, Yu, T., & Li, P. (2017). Comparative study of daytime and nighttime sap flow of
909 *Populus euphratica*. *Plant Growth Regulation*, 82, 353-362. <https://doi.org/10.1007/s10725-017-0263-6>
- 910 Zweifel, R. (2016). Radial stem variations – a source of tree physiological information not fully exploited yet.
911 *Plant Cell and Environment*, 39, 231-232. <https://doi.org/10.1111/pce.12613>

- 912 Zweifel, R., &Häsler, R. (2001). Dynamics of water storage in mature subalpine Piceaabies: temporal and
913 spatial patterns of change in stem radius. *Tree Physiology*, 21(9), 561-
914 569.<https://doi.org/10.1093/treephys/21.9.561>
- 915 Zweifel, R., Item, H., &Häsler, R. (2000). Stem radius changes and their relation to stored water in stems of
916 young Norway spruce trees. *Trees*, 15, 50-57. <https://doi.org/10.1007/s004680000072>
- 917 Zweifel, R., Item, H., &Häsler, R. (2001). Link between diurnal stem radius changes and tree water relations.
918 *Tree Physiology*, 21(12-13), 869-877. <https://doi.org/10.1093/treephys/21.12-13.869>
- 919 Zweifel, R., Zimmermann, L., & Newbery, D. M. (2005). Modeling tree water deficit from microclimate: an
920 approach to quantifying drought stress. *Tree Physiology*, 25(2), 147-156.
921 <https://doi.org/10.1093/treephys/25.2.147>